SUPERSONIC SOURCE FLOW PAST THIN AIRFOILS

Thesis by

Bernard Rasof

In Partial Fulfillment of the Requirements

For the Degree of

Doctor of Philosophy

California Institute of Technology

Pasadena, California

1950

ACKNOWLEDGEMENTS

The writer is indebted to Professor H. J. Stewart for his encouragement and valuable assistance during the preparation of this thesis. Dr. Morton Alperin has been very generous with helpful advice and discussions.

Miss Alberta Pampeyan typed the manuscript with patience and care.

ABSTRACT

In this thesis the supersonic source flow over a thin sharp-edged airfoil is formulated as a linearized problem. A new potential equation is derived, using a system of spherical coordinates centered at the source; as a simplification only wings symmetrical about the z axis are considered, and of these only the limiting cases of ring- and annular- airfoils are treated.

After transforming to characteristic coordinates in the hodograph plane, the potential equation (which has variable coefficients) is shown to be approximated by two classical equations -- one holding for the ring wing and the other applying to the annular wing. The flow over a specific annular wing is computed by an application of the Riemann method to the telegraph equation, which is the appropriate approximation to the governing equation for this case.

The linearized potential equation is also solved by the Method of Characteristics, using a numerical equivalent of the Monge procedure for quasilinear partial differential equations. A complete set of compatibility equations is exhibited, allowing the computation of the perturbation velocity components at any point of the zone of influence of an airfoil set in the supersonic source flow. Two numerical examples are presented, illustrating the application to the computation of the flow over each of a ring- and annular- wing.

Finally, in an appendix the usually powerful method of separation of variables is shown to be unsuitable as a procedure for solving the potential equation governing the present problem.

TABLE OF CONTENTS

I. INTRODUCTION

1. An important restriction of conventional wing theory is the assumed uniformity of the undisturbed flow in which the airfoil is immersed.

The assumption of uniform flow is not valid in several important cases, of which obvious instances are

a) a wing spanning an open jet wind tunnel,

b) a wing in a propeller slipstream,

c) a tail surface behind a supersonic wing.

To solve problems such as these several authors (Refs. 1, 2, 3) have modified the existing standard wing theory by weakening or discarding the hypothesis of strictly uniform flow.

However, studies of non-uniform flow generally have retained the assumption of rectilinear motion of the undisturbed fluid: for subsonic flow the streamlines are presumed parallel at infinity, and in all of the supersonic cases, including the flow about yawed pointed bodies of revolution (Refs. 4, 5, 6, 7), the streamlines are assumed to be parallel up to the zone of influence of the obstructing body, although the flow between the attached shock front and a yawed pointed body of revolution is not rectilinear.

2. One of the reasons for this general attention to rectilinear undisturbed flows is a consequence of the most important application of supersonic flow theory, which is to the design of aircraft expected to fly at supersonic speeds through a relatively motionless atmosphere.

Since the viewpoint that the aircraft has a supersonic speed in still air is equivalent to that in which the aircraft is at rest in an air flow moving at the same but oppositely signed speed, it is reasonable to assume that when the air stream enters the zone of influence of the aircraft it has a uniform velocity which is the negative of the actual velocity of the aircraft. Thus, for the aeronautical engineer, rectilinear flows are the most significant.

The consideration of rectilinear flows is also attractive for the reason that in this case the linearized differential equation satisfied by the perturbation potential has constant coefficients and is relatively easy to solve. When the undisturbed flow is not rectilinear the analogous perturbation potential equation will have variable coefficients.

Furthermore, for the most exhaustively explored problem -- two dimensional linearized supersonic airfoils in a uniform rectilinear supersonic flow -- it is very easy to satisfy the boundary condition of outgoing waves by choosing one of the two general solutions of the governing differential equation to stand for each of the two surfaces. In general the condition of outgoing waves cannot be satisfied in this simple manner, and this is another of the reasons why the theory of airfoils in other than rectilinear flows has not been pursued.

3. Of problems in the supersonic flow of a fluid over a submerged object, in which it is not possible to ascribe a rectilinear motion to the undisturbed stream, perhaps the one of most practical importance is the case in which the gaseous combustion products of a rocket are

exhausted past a small wing or vane (Fig. 1). Such a wing would

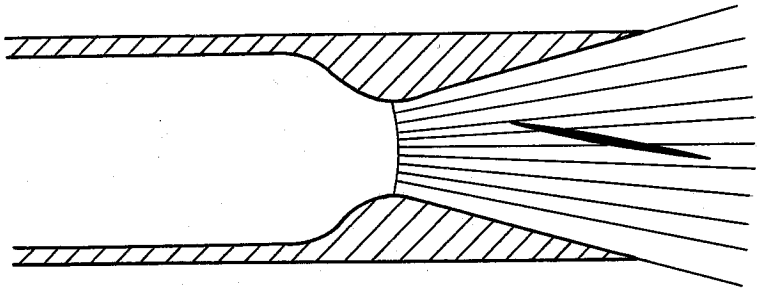

Fig. 1 - A Small Supersonic Wing in a Rocket Nozzle

function to deflect the exhaust gases from their initially undisturbed direction, causing a nonsymmetrical flow; the component of the resultant force normal to the motor axis would act to deflect the rocket, or any rigidly attached vehicle, from its course. In this way, a small wing set in a rocket exhaust could be the means of controlling the flight of a rocket powered aircraft.

4. In its most highly developed form, the theory of steady compressible fluid flow is based on the following assumptions:

a) The effect of body forces can be neglected,

b) No heat is added to or subtracted from any portion of the fluid,

c) Within the streaming fluid the thermal processes are isentropic,

d) The working fluid is a perfect gas,

e) The viscosity is zero,

f) The undisturbed flow is initially irrotational,

g) Before entering the zone of influence of a small obstruction the fluid has a uniform, rectilinear motion,

h) An obstacle in the stream changes the velocities in the undisturbed fluid only slightly.

In the present problem, in which the rocket exhaust is the primary flow, all of these assumptions, with the exception of (g), will be retained.* In place of (g) the motion of the gas forming the rocket exhaust is now assumed to be approximated to by a supersonic source flow.

Thus, this thesis has for its purpose the calculation of the steady flow field downstream of a small wing, set at a slight angle of attack, in a non-viscous, non-heat conducting, compressible supersonic perfect gas issuing isentropically, without rotation, from a source.

5. The equations governing the steady motion of a non-viscous, non-conducting compressible perfect gas, free of body forces, and subject to only isentropic processes are

$$\bar{q} \cdot \nabla \bar{q} = -\frac{1}{\rho} \nabla p \tag{1.1}$$

$$\nabla \cdot (\rho \bar{q}) = 0 \tag{1.2}$$

$$p = \kappa \rho^{\gamma} \tag{1.3}$$

---

* Underlying (c) is the assumption that the working fluid is a homogeneous system of non-reacting fluids, which will be true if the combustion is completed in the rocket chamber. This is certainly not the case for present day rockets. However, in the history of Fluid Mechanics, the introduction of new features in the subject has had to be balanced by simplifications in another direction. There are enough inherent difficulties in treating a problem in non-uniform flow without adding to the complications by discarding the simplifying assumption of isentropic flow. Further, any other postulated thermal process probably would be no more accurate than that of isentropic flow; hence, in the present investigation, the thermal processes will be assumed to have their simplest nature, given in (c).

where $\rho, p, \bar{q}$ are respectively the local density, pressure and velocity at a point in the fluid, K is a constant, and γ is the (constant) ratio of the two specific heats of the gas.

For an isentropic process,

$$\nabla p = a^2 \nabla \rho, \tag{1.4}$$

where a is the speed with which an infinitesimal disturbance is propagated in the fluid.

Combining all three of (1.1), (1.2), (1.3) and making use of (1.4), it is seen that the motion of the fluid is described by the single (scalar) equation

$$\bar{q} \cdot [\bar{q} \cdot \nabla \bar{q}] = a^2 \nabla \cdot \bar{q}. \tag{1.5}$$

The assumption of irrotationality is now employed, for the purpose of which it is helpful to put equation (1.5) into a more convenient form by use of the identity

$$\tfrac{1}{2} \nabla (\bar{q} \cdot \bar{q}) \equiv \bar{q} \cdot \nabla \bar{q} + \bar{q} \times (\nabla \times \bar{q}). \tag{1.6}$$

Setting (1.6) into (1.5) results in

$$\tfrac{1}{2} \bar{q} \cdot [\nabla (\bar{q} \cdot \bar{q}) - 2 \bar{q} \times (\nabla \times \bar{q})] = a^2 \nabla \cdot \bar{q}. \tag{1.7}$$

The postulate of no rotation implies that the velocity components can be obtained as derivatives of a single-valued potential function Φ, or that

$$\bar{q} = \nabla \Phi.$$

Since $\bar{q}$ is now the gradient of a scalar, the term $\bar{q} \times (\nabla \times \bar{q})$ in (1.7) vanishes, and that equation takes the form

$$\tfrac{1}{2} \nabla \Phi \cdot [\nabla \ \nabla \Phi \cdot \nabla \Phi] = a^2 \nabla^2 \Phi, \tag{1.8}$$

the "potential equation" of motion of a perfect compressible fluid.

In general orthogonal curvilinear coordinates q_1, q_2, q_3 equation (1.8) becomes

$$\sum_{i=1}^{3}\sum_{j=1}^{3} \frac{1}{Q_i^2 Q_j^2} \frac{\partial \Phi}{\partial q_i} \frac{\partial \Phi}{\partial q_j} \left[\frac{\partial^2 \Phi}{\partial q_i \partial q_j} - \frac{1}{Q_j} \frac{\partial Q_j}{\partial q_i} \left(\frac{\partial \Phi}{\partial q_j} \right)^2 \right] =$$

$$\frac{a^2}{Q_1 Q_2 Q_3} \left[\frac{\partial}{\partial q_1} \left(\frac{Q_2 Q_3}{Q_1} \frac{\partial \Phi}{\partial q_1} \right) + \frac{\partial}{\partial q_2} \left(\frac{Q_3 Q_1}{Q_2} \frac{\partial \Phi}{\partial q_2} \right) + \frac{\partial}{\partial q_3} \left(\frac{Q_1 Q_2}{Q_3} \frac{\partial \Phi}{\partial q_3} \right) \right],$$

where

$$Q_K^2 = \left(\frac{\partial x}{\partial q_K} \right)^2 + \left(\frac{\partial y}{\partial q_K} \right)^2 + \left(\frac{\partial z}{\partial q_K} \right)^2, \quad K = 1, 2, 3,$$

are the coefficients of the line element of arc length in the orthogonal q_1, q_2, q_3 space.

II. PURE SUPERSONIC SOURCE FLOW OF A PERFECT COMPRESSIBLE FLUID

6. The coordinate system appropriate to a source flow is that one called spherical (Fig. 2), for which the equations of transformation

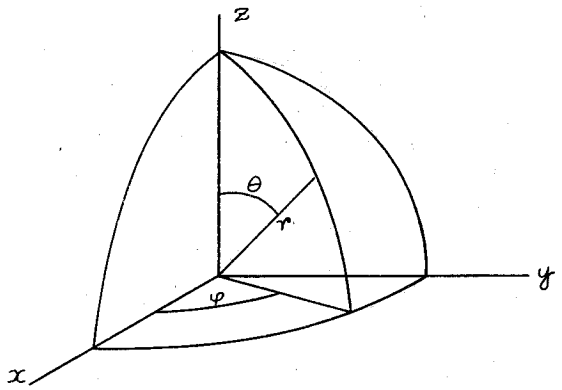

Fig. 2 - Spherical Polar Coordinates

to cartesian coordinates are given by

$$\begin{aligned} x &= r \sin\theta \cos\varphi \\ y &= r \sin\theta \sin\varphi \\ z &= r \cos\theta. \end{aligned} \tag{2.1}$$

Referred to spherical polar coordinates r, θ, φ the potential equation of motion (1.8) becomes, with the use of (2.1),

$$\begin{aligned} &(a^2 - \Phi_r^2)\Phi_{rr} + \left(a^2 - \frac{\Phi_\theta^2}{r^2}\right)\frac{\Phi_{\theta\theta}}{r^2} + \left[a^2 - \frac{\Phi_\theta \Phi_{r\theta}}{r} + \frac{\Phi_\theta^2}{2r^2}\right]\frac{2}{r}\Phi_r + a^2\frac{\cot\theta}{r^2}\Phi_\theta + \\ &\left(a^2 - \frac{\Phi_\varphi^2}{r^2\sin^2\theta}\right)\frac{\Phi_{\varphi\varphi}}{r^2\sin^2\theta} + \left[\frac{\Phi_r}{r} + \frac{\cos\theta}{r^2\sin^2\theta}\Phi_\theta\right]\frac{\Phi_\varphi^2}{r^2\sin^2\theta} - 2\left[\Phi_r\Phi_{r\varphi} + \frac{\Phi_\varphi\Phi_{\theta\varphi}}{r^2\sin\theta}\right]\frac{\Phi_\varphi}{r^2\sin^2\theta} = 0. \end{aligned} \tag{2.2}$$

7. In Hydrodynamics a source is a hypothetical point from which fluid is imagined to issue uniformly with regard to direction; on each sphere centered at the source the fluid properties are constant, depending only on the radius. To deduce the velocities, pressures, etc., at any point in the field of a perfect compressible fluid welling from a source, the potential of (2.2) is specialized to $\phi(r)$, where r is the distance from the source, resulting in the equation

$$\left[\phi'^2(r) - a_s^2(r)\right]\phi''(r) - \frac{2}{r}\, a_s^2(r)\,\phi'(r) = 0. \tag{2.3}$$

Another form of the potential equation (2.3) which is convenient for later use is obtained by introducing into that equation the local Mach number in the source flow,

$$M_s(r) = \frac{\phi'(r)}{a_s(r)},$$

leading to

$$\left[M_s^2(r) - 1\right]\phi''(r) - \frac{2}{r}\,\phi'(r) = 0. \tag{2.4}$$

A third form of the potential equation of motion of a supersonic compressible source flow is obtained by consideration of the energy equation, which here has the form

$$a_s^2(r) = a_0^2 - \frac{\gamma-1}{2}\,\phi'^2(r), \tag{2.5}$$

where a_0 is the speed of sound in the fluid at stagnation conditions and is constant when the flow field is isentropic. Substitution of (2.5) into (2.3) results in

$$\left[V^2(r) - \lambda^2\right]V'(r) - \frac{2\lambda^2}{r}\,V(r)\left[1 - V^2(r)\right] = 0, \tag{2.6}$$

where $V(r) \equiv \phi'(r)/c$, in which c is the maximum possible speed the fluid can attain (at $r = \infty$) and $\lambda^2 = \frac{\gamma-1}{\gamma+1}$, a constant.

8. Equation (2.6) can be integrated to

$$r^2 V(r)\left[1-V^2(r)\right]^{\frac{2}{\gamma-1}} = A_1^2, \qquad (2.7)$$

where A_1 is a constant of integration, which is essentially the continuity equation. A more convenient form of (2.7) is obtained by using the "critical speed of sound", at which the local fluid and sound speeds have a common value a_*, to construct the dimensionless speed ratio

$$M_s^*(r) \equiv \phi'(r)/a_* = V(r)/\lambda, \qquad (2.8)$$

called the "critical Mach number".*

The use of a_* rather than some other quantity which is constant in the entire flow field, say a_0, is justified on the basis that it is the cut which separates the subsonic and supersonic speeds, for by definition

the flow is subsonic when $0 \leq \phi'(r) < a_*$

the flow is supersonic when $a_* < \phi'(r)$.

After substituting (2.8) into (2.7) and rearranging, there results

$$\frac{r}{A} = M_s^{*-1/2}(r)\left[1-\lambda^2 M_s^{*2}(r)\right]^{-\frac{1}{2(\gamma-1)}}, \qquad (2.9)$$

where $A^2 \equiv A_1^2/\lambda$. For air at ordinary conditions $\gamma = 1.40$ and $\lambda^2 = 1/6$, so

$$\left(\frac{r}{A}\right)_{air} = M_s^{*-1/2}(r)\left[1-\tfrac{1}{6}M_s^{*2}(r)\right]^{-1.25}. \qquad (2.9)a$$

---

* Since a_* is a constant for the entire field of flow, $M_s^*(r)$ is directly proportional to the local fluid speed; on the other hand, $M_s(r)$ is a complicated function of r.

A graphical representation of formula (2.9)a is given in Fig. 3.

9. From the elementary theory of maxima and minima it is easy to see that for any value of λ the right hand member of (2.9) has a real minimum when $M_s^*(r)$ is unity, or, using (2.8), when $v = \lambda$. The minimum value of $\frac{r}{A}$ is given by

$$\left(\frac{r}{A}\right)_{min.} = \left(\frac{\gamma+1}{2}\right)^{\frac{1}{2(\gamma-1)}} ;$$

thus, there is a spherical boundary on which the local speed of the fluid is sonic, and the supersonic flow outside of the sphere cannot be continued into the interior.

This same result could have been forseen from an examination of (2.4), for $M_s(r)=1$ is a regular singular point of the differential equation, and thus there are two solutions, one in the range $M_s(r)>1$ and another in the range $0 \leq M_s(r) < 1$; one solution cannot be continued analytically into the other.

10. The well known relations (Ref. 8, p. 25) between the critical and local Mach numbers become, for the source flow,

$$M_s^{*2}(r) = \frac{1}{\lambda^2 + \frac{2}{\gamma+1}\frac{1}{M_s^2(r)}} \tag{2.10}$$

and

$$M_s^2(r) = \frac{2}{\gamma+1}\frac{M_s^{*2}(r)}{1-\lambda^2 M_s^{*2}(r)} . \tag{2.11}$$

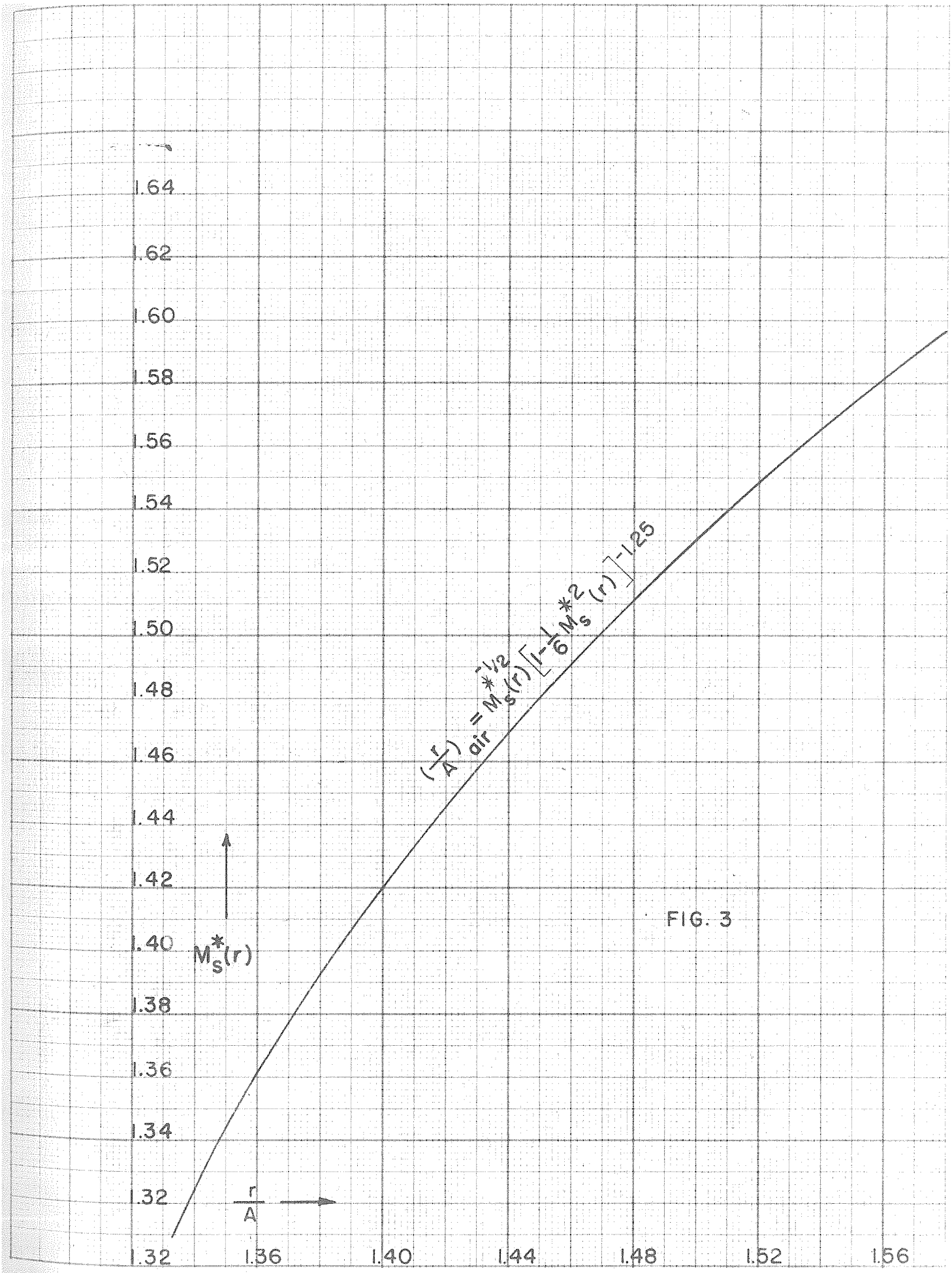
1.64
1.62
1.60
1.58
1.56
1.54
1.52
1.50
1.48
1.46
1.44
1.42
1.40
1.38
1.36
1.34
1.32
$M_s^*(r)$
$\frac{r}{A}$
1.32
1.36
1.40
1.44
1.48
1.52
1.56
$(\frac{r}{A})_{air} = M_s^*(r)\left[1-\frac{1}{6}M_s^{*2}(r)\right]^{-1.25}$

FIG. 3

11. For the purpose of calculating pressures in the compressible source flow field, the relation (2.9) is rewritten as

$$\frac{A/r}{M_s^{*1/2}(r)} = \left[1-\lambda^2 M_s^{*2}(r)\right]^{\frac{1}{2(\gamma-1)}}. \qquad (2.9)'$$

Since the working fluid has been assumed to be a perfect gas subjected to only isentropic changes, the pressure ratio p_s/p_o has the form (Ref. 8, p. 26)

$$\frac{p_s}{p_o} = \left[1-\lambda^2 M_s^{*2}(r)\right]^{\frac{\gamma}{\gamma-1}}. \qquad (2.12)$$

Then, comparing (2.9)' and (2.12), the pressures in the compressible source flow are seen to be given by the formula

$$\frac{p_s}{p_o} = \left[\frac{(A/r)^2}{M_s^*(r)}\right]^{\gamma}. \qquad (2.13)$$

The values of $M_s^*(r)$ corresponding to a given $\frac{r}{A}$ for $\gamma=1.40$ are obtained from Fig. 3.

The dynamic pressure in the source flow,

$$q_s = \tfrac{1}{2}\rho_s \phi'^2(r),$$

can be rewritten as

$$q_s = \tfrac{1}{2}\gamma p_s M_s^{*2}(r),$$

or, using (2.11) and (2.12), as

$$\frac{q_s}{p_s} = \frac{\gamma}{\gamma+1}\,\frac{M_s^{*2}(r)}{1-\lambda^2 M_s^{*2}(r)}. \qquad (2.14)$$

III. RESTRICTION TO AXIALLY - SYMMETRIC MOTIONS AND LINEARIZATION OF THE RESULTING EQUATION

12. Now it is assumed that a wing is set into the perfect, irrotational compressible fluid issuing from the supersonic source. In the zone of influence, the part of the flow field to which are confined the disturbances due to the wing, the fluid motion is deranged from the strictly radial stream which is the mark of a purely source flow. Instead, in the general case, throughout the action zone the motion of the fluid can be described only as a function of three independent space variables.

Problems in the three dimensional motion of a perfect fluid possess great inherent difficulties, due primarily to the complexity of the differential equations, which for steady flows have three independent variables. Steady, supersonic plane potential rectilinear flows can be reduced to the discussion of the two-dimensional wave equation, which has been intensively studied, but for general three-dimensional problems no such highly developed mathematical structure exists.

Thus, it is appropriate to reduce the mathematical difficulties by consideration of a special case of the general three-dimensional problem.

As a first approach to the spatial source-wing problem the case in which the deranged flow caused by the wing is symmetrical about one of the cartesian axes, say the z-axis, will be investigated. Then, in all planes containing the (z) axis of symmetry the flow will be the same; such planes are defined by the coordinate φ hence the fluid motion will be independent of φ and can be studied in any one

meridinal plane.

In the sequel attention will be confined to such axially symmetric flows, for which the potential Φ of (2.2) is specialized to $\Phi(r,\theta)$, causing that equation to assume the form

$$\left(a^2-\Phi_r^2\right)\Phi_{rr} - 2\frac{\Phi_r\Phi_\theta}{r}\frac{\Phi_{r\theta}}{r} + \left(a^2-\frac{\Phi_\theta^2}{r^2}\right)\frac{\Phi_{\theta\theta}}{r^2} + 2\frac{a^2}{r}\Phi_r + a^2\frac{\cot\theta}{r^2}\Phi_\theta + \frac{\Phi_r\Phi_\theta^2}{r^3} = 0. \qquad (3.1)$$

13. The present state of mathematical knowledge does not include a general approach toward an exact solution of the highly non-linear partial differential equation (3.1), representing the axially-symmetric disturbed source flow of a perfect compressible fluid past a wing which so alters the velocities that no longer can they be derived from the simple potential of the source.

However, the changes in velocity will not be large when the airfoil is thin, with sharp leading and trailing edges, and the angle of attack is small. For many similar situations in the theory and practice of the high speed flow of compressible fluids it is not the velocity of the fluid (or the velocity potential, the rigorous solution of the potential equation of motion from which the velocity can be derived) which is of interest, so much as the variations produced in the velocity of the undisturbed flow by obstacles in the stream. Such attention to the "velocity perturbations" rather than to the velocities themselves leads to an elegant method of investigating the consequence of a small obstruction set in a moving fluid possessing a simple flow pattern. Many important aeronautical problems are approximated by this combination of small obstacle and simple flow.

This notion of concentrating on the slight changes produced in the flow pattern by a weak disturbance, rather than attempting to determine the character of the existing deranged flow, is the basis of the "method of small perturbations." In the present investigation this method can be employed, since the wing will be supposed thin, with sharp leading and trailing edges, set at a slight angle of attack to the flow. Presuming such a diminutive wing, with consequent small disturbance to the source flow, the non-linear differential equation (3.1) can be linearized after restating the supposition of a small wing in the following way:

> It is assumed that compared to the local velocity $\phi'(r)$ of the main (source) flow the local changes in the velocity components provoked by the wing are so small that they can be regarded as perturbations added to the primary velocity.

14. A thin, sharp edged wing will cause an axially symmetric flow slightly deranged from the original source flow when it has axial symmetry and is approximately on the lateral surface of a right circular truncated cone with vertex at the source (see Fig. 4).

There are two extreme cases, distinguished by the order of magnitude of the coordinate θ. When θ is small, of the order of 6° or so, the airfoil will be called a ring wing -- here it is not important whether the surface from which the ring wing departs slightly is considered to be the lateral surface of a cone or the lateral surface of a right circular cylinder with z as its axis of symmetry (see Fig. 5). On the other hand, when θ is close to $\frac{\pi}{2}$ the airfoil will be called an

annular wing -- here the proper surface to use in approximations is the x, y plane (see Fig. 6).

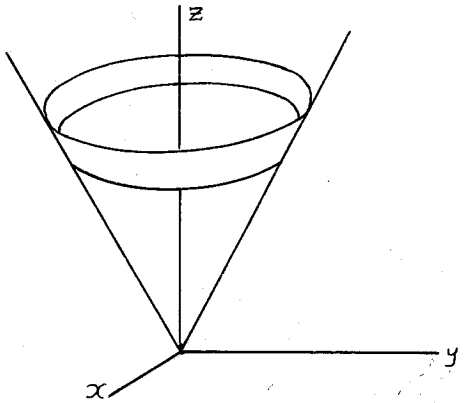

Fig. 4 - Truncated Conical Airfoil in a Supersonic Source Flow

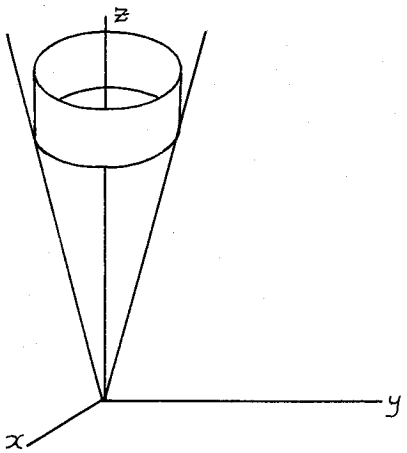

Fig. 5 - Ring Wing in a Supersonic Source Flow

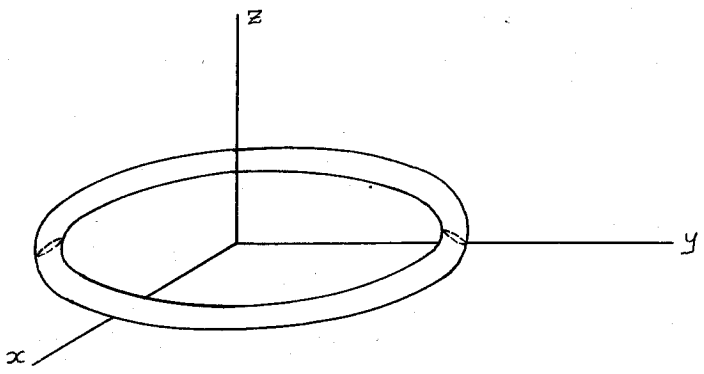

Fig. 6 - Annular Wing in a Supersonic Source Flow

For other truncated conical wings the coordinate θ will have values intermediate between "small" and "close to $\frac{\pi}{2}$ ". It will be seen later that when θ is small or close to $\frac{\pi}{2}$ it is possible to justify certain simplifying approximations, and hence it is convenient to restrict the airfoils in the source flow to just the ring and annular wings. The general case of the truncated cone wing will not be considered.

This investigation may be applied to a small wing, and hence so far as the annular wing is concerned the interest here is in a part of the annulus cut out by two planes normal to the x, y plane. The particular shape of the tips is not important, because the theory is only able to account for the flow over the central portion of the wing, between the Mach cones which have their vertices at the outermost point on the leading edge (Fig. 7).

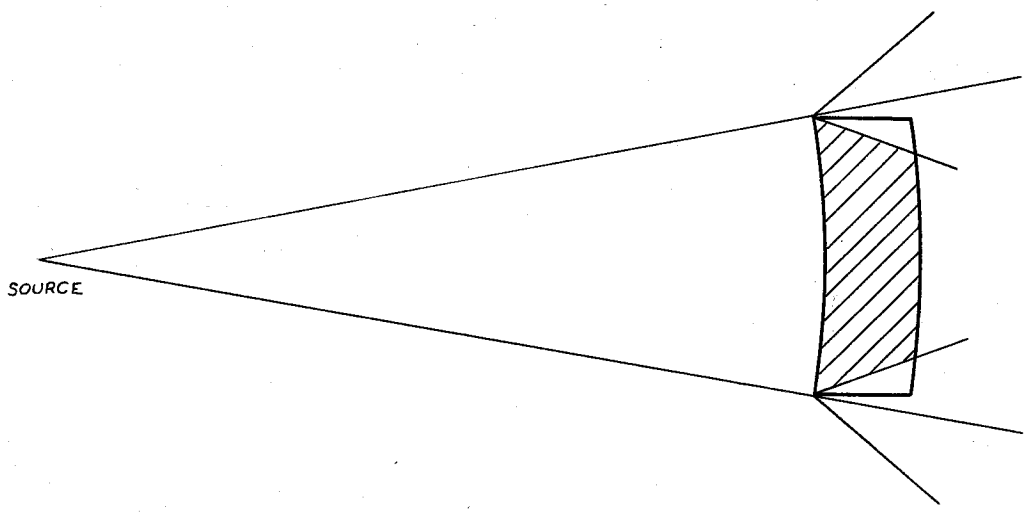

Fig. 7 - Planform of an Annular Wing. The Theory Neglects Tip Effects and so can be Applied only to the Shaded Portion.

For the ring wing, it is clear that in all planes containing the z-axis (of symmetry) the streamline patterns will be identical. However, for the annular wing as delineated above, in half planes which begin at the z-axis the flow will be of two types, depending on whether or not the plane cuts the central part of the wing, between the Mach cones due to the tips:

a) When the half plane intersects the shaded portion of the wing: - supersonic fluid motion axially-symmetrically perturbed from the source flow due to the presence of the wing.

b) When the half plane does not intersect the shaded portion of the wing: - disturbed supersonic source flow with no axial-symmetry.

Case (a) only is of interest, because here the flow is deranged in an axially symmetric way from its initially simple character. Again, in all planes which are interrupted by the shaded portion of the wing the fluid motions are identical and independent of the coordinate φ defining the plane, requiring examination in only one such plane.

15. The purely source flow is obviously irrotational, and in section 4 the thermal processes were assumed to be isentropic, which means that the fluid pressure is a function of the density only, and so the Lagrange theorem (Ref. 9), that a perfect fluid in irrotational motion remains permanently without rotation, holds. Thus, since a velocity potential exists for every portion of the undisturbed source flow, the disturbed fluid also possesses a velocity potential, which may be identified with $\Phi(r,\theta)$ of Eq. (3.1).

In the silent zone the velocities can be derived from the simple

velocity potential of a compressible source, while in the action zone the flow patterns are deranged by reason of the disturbing influence of the wing. Hence, in the actual existing flow, in the zone of influence, the velocities differ fundamentally from those in the pure source flow.

However, by assuming that the disturbing effect of the wing is small -- that is, by postulating that in the zone of influence the streamline pattern differs only slightly from the compressible source flow which would there exist but for the wing -- it is possible to employ the method of perturbations to calculate approximately the disturbed fluid motion. With this supposition of slight distortion, the velocity potential of the actual flow is assumed to be a linear combination of two potentials:

1) $\phi(r)$, representing the main (source) flow, and

2) $\varepsilon(r,\theta)$, a "perturbation potential", characterizing the amount by which the wing distorts the primary flow.

Than is, the small wing is mathematically introduced into the flow governed by Eq. (3.1) when the velocity potential is taken to be

$$\Phi(r,\theta) = \phi(r) + \varepsilon(r,\theta). \qquad (3.2)$$

The velocity components ε_r and $\frac{1}{r}\varepsilon_\theta$, representing the wing, as well as their derivatives, are assumed to be small, so that products of the perturbed velocities with one another and with their derivatives will be neglected in comparison with the first order terms, and hence the theory subsequently developed is a first approximation to the actual state of affairs.

For consistency, the speed of sound $a(r,\theta)$ in the perturbed flow

must be written in a linearized form; when the undisturbed fluid is a supersonic source flow the linearized speed of sound is

$$a^2(r,\theta) = a_s^2(r) - (\gamma-1)\,\phi'(r)\,\varepsilon_r. \tag{3.3}$$

When (3.2) and (3.3) are set into equation (3.1), after discarding the zero order terms, which vanish identically by (2.3), and retaining only first order terms in the perturbation velocities, there remains

$$\left[a_s^2(r)-\phi'^2(r)\right]\varepsilon_{rr} + a_s^2(r)\frac{\varepsilon_{\theta\theta}}{r^2} + \left[\frac{2}{r}\left\{a_s^2(r)-(\gamma-1)\,\phi'^2(r)\right\} - (\gamma+1)\,\phi'(r)\,\phi''(r)\right]\varepsilon_r + a_s^2(r)\frac{\cot\theta}{r^2}\,\varepsilon_\theta = 0. \tag{3.4}$$

The coefficient of ε_r in (3.4) can be put into a more convenient form, for from (2.3),

$$\phi'(r)\,\phi''(r) = \frac{2a_s^2(r)}{r}\,\frac{\phi'^2(r)}{\phi'^2(r)-a_s^2(r)},$$

and so

$$\frac{2}{r}\left\{a_s^2(r)-(\gamma-1)\,\phi'^2(r)\right\} - (\gamma+1)\,\phi'(r)\,\phi''(r) = -\frac{2}{r}\,\frac{(\gamma-1)M_s^4(r)+M_s^2(r)+1}{M_s^2(r)-1}. \tag{3.5}$$

After multiplication of (3.4) by r^2 and the use of the right hand member of (3.5) as the coefficient of ε_r the final form of the linearized equation of motion is obtained:

$$r^2\left[M_s^2(r)-1\right]\varepsilon_{rr} - \varepsilon_{\theta\theta} + 2r\,\frac{(\gamma-1)M_s^4(r)+M_s^2(r)+1}{M_s^2(r)-1}\,\varepsilon_r - \cot\theta\,\varepsilon_\theta = 0. \tag{3.6}$$

16. From physical considerations, when a solid body is set into the supersonic source flow, the resulting disturbed fluid motion must satisfy the following boundary conditions:

a) Where the body exists the perturbation velocity vector, with

components $(\varepsilon_r, \varepsilon_\theta/r)$, is tangent to the surface;

b) The perturbation velocities vanish identically upstream of (and on) the spherical surface,* centered at the source and lying wholly in the field of supersonic flow, which passes through the leading edge of the body; and a related condition,

c) Waves leaving the surface must be outgoing; that is, must be directed downstream of the body.

If OA in Fig. 8 is a streamline from the origin of the coordinate system (the source) to a point A on either the ring or annular airfoils,

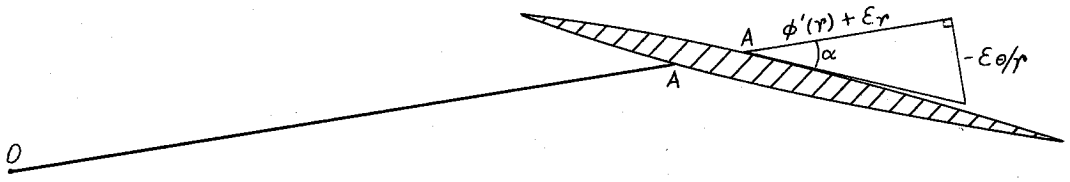

Fig. 8

then, whether A is on the upper or lower surface, the velocity components in the disturbed flow will be

$\phi'(r) + \varepsilon_r$ in the radial direction, and

$-\varepsilon_\theta/r$ in the angular direction.

Hence, if α is the angle of attack of the surface at A to the primary source flow,

$$\tan \alpha = -\frac{\varepsilon_\theta/r}{\phi'(r) + \varepsilon_r}$$

---

* In a plane of symmetry the trace of this spherical surface will be an arc of a circle.

or

$$+\varepsilon_\theta/r = -\phi'(r)\tan\alpha. \qquad (3.7)$$

Thus the boundary condition (a) is expressed in the form of a condition on the velocity perturbation in the angular direction.

17. Summarizing, the boundary value problem which describes the fluid motion deranged from the basic source flow due to the presence of (either a ring- or annular-wing can be formulated as follows: The governing differential equation is

$$r^2\left[M_s^2(r)-1\right]\varepsilon_{rr} - \varepsilon_{\theta\theta} + 2r\,\frac{(\gamma-1)M_s^4(r)+M_s^2(r)+1}{M_s^2(r)-1}\,\varepsilon_r - \cot\theta\,\varepsilon_\theta = 0$$

and the boundary conditions are given by

a) $\varepsilon_\theta/r = -\phi'(r)\tan\alpha$;

b) (In any plane of symmetry) ε_r and ε_θ/r vanish identically on a circular arc, with center at the source, which passes through the leading edge of the airfoil; and a related condition,

c) Waves leaving the body must be directed downstream.

A boundary value problem in which the partial differential equation is hyperbolic possesses a unique solution if three conditions -- one on a time-like curve and two on a space-like curve -- are prescribed (Ref. 10, p. 85). A direction is called time-like if it separates the characteristics; the surface of the airfoil is such a time-like direction, and one datum (a), is prescribed there. If both characteristics through a given point lie on one side of a given curve that curve is called space-like. Clearly, the circular arc, centered at the source, which passes through the leading edge of the airfoil,

is space-like; and on this curve two conditions (b), on ε_r and ε_θ/r, are prescribed.

Thus, the three conditions of (a) and (b) are sufficient to provide a unique solution to the boundary value problem describing the axially symmetric disturbed flow which is the result of introducing a thin supersonic ring- or annular-wing, at a slight angle of attack, into a supersonic source flow.

18. When the perturbation potential $\varepsilon(r,\theta)$ of equation (3.6) is known, the perturbation velocities, and hence the local fluid pressures, can be calculated.

For the purpose of determining the pressures in the field of perturbed flow it is convenient to first define

$\frac{\varepsilon_r}{a_*} \equiv m_r^*$ to be the radial component of the perturbation in the source flow critical Mach number $M_s^*(r)$, and

$\frac{\varepsilon_\theta/r}{a_*} \equiv m_\theta^*$ to be the angular component of the perturbation in the source flow critical Mach number $M_s^*(r)$.

Retaining only first order terms, the critical Mach number M^* of the perturbed flow is related to $M_s^*(r)$ by

$$M^* = M_s^*(r)\left[1 + m_r^*/M_s^*(r)\right]. \tag{3.8}$$

Since the flow is isentropic, the local pressure p in the deranged flow is given by (Ref. 8, p. 26)

$$p = p_0\left[1-\lambda^2 M^{*2}\right]^{\frac{\gamma}{\gamma-1}}. \tag{3.9}$$

Setting (3.8) into (3.9) and linearizing, there remains

$$p = p_s \left[1 - \frac{2\gamma}{\gamma+1} \frac{M_s^{*}(r)}{1-\lambda^2 M_s^{*2}(r)} m_r^{*} \right], \tag{3.10}$$

where p_s is the local pressure in the source flow, given by equation (2.12).

19. By introducing an airfoil into a supersonic source flow, a pressure coefficient c_{p_s} can be defined as

$$c_{p_s} = \frac{p - p_s}{q_s}, \tag{3.11}$$

where q_s is the local dynamic pressure in the primary source flow, given in equation (2.14).

From the definition (3.11), using (3.10) and (2.14),

$$c_{p_s} = -2 \frac{m_r^{*}}{M_s^{*}(r)}, \tag{3.12}$$

which is identical in form with the pressure coefficient for uniform rectilinear isentropic flow.

20. The pressure coefficient calculated from (3.13) will be compared with the pressure coefficient for "linearized locally rectilinear flow", where the formulas of rectilinear supersonic flow theory are employed. Thus, when a wing is set into a supersonic source flow the critical Mach number of the perturbed flow is given by linearized locally rectilinear flow theory as

$$M^{*} = M_s^{*} \pm \frac{M_s^{*}(r) \tan\alpha}{\sqrt{M_s^2(r) - 1}}, \tag{3.13}$$

where α is the angle of attack of the airfoil surface and the (+) and (-) signs are used with the upper and lower surfaces, respectively.

From (Ref. 8, p. 145) the pressure coefficient for linearized rectilinear flow has the value

$$C_{p_r} = - \frac{2 \tan \alpha}{\sqrt{M_3^2(r) - 1}} . \qquad (3.14)$$

IV. REDUCTION OF THE PERTURBATION POTENTIAL EQUATION TO CERTAIN CLASSICAL FORMS. APPLICATION TO A NUMERICAL EXAMPLE.

21. The fundamental equation (3.6) can be condensed to

$$\frac{\partial}{\partial r}\left[r^2\left\{M_s^2(r)-1\right\}\varepsilon_r\right] - 2rM_s^2(r)\varepsilon_r - \frac{1}{\sin\theta}\frac{\partial}{\partial\theta}\left(\varepsilon_\theta \sin\theta\right) = 0, \tag{4.1}$$

and then further reduced by writing the coefficients in terms of the potential $\phi'(r)$ representing the supersonic source flow. From equation (2.4),

$$r^2\left[M_s^2(r)-1\right] = 2r\,\frac{\phi'(r)}{\phi''(r)}$$

and

$$2rM_s^2(r) = 2\left[r + 2\,\frac{\phi'(r)}{\phi''(r)}\right],$$

so equation (4.1) becomes

$$\frac{\partial}{\partial r}\left[r\,\frac{\phi'(r)}{\phi''(r)}\,\varepsilon_r\right] - \left(r+2\,\frac{\phi'(r)}{\phi''(r)}\right)\varepsilon_r - \frac{1}{2\sin\theta}\frac{\partial}{\partial\theta}\left(\varepsilon_\theta\sin\theta\right) = 0. \tag{4.2}$$

In the hodograph plane, with independent variables (V, θ), where $V(r) \equiv \phi'(r)/c$, the differential equation (4.2) has the form

$$rV(r)V'(r)\,\varepsilon_{vv} - V\varepsilon_v - \frac{1}{2\sin\theta}\frac{\partial}{\partial\theta}\left(\varepsilon_\theta\sin\theta\right) = 0. \tag{4.3}$$

By again using the potential equation of the source flow, this time in the form (2.6), from which

$$rV(r)V'(r) = 2\lambda^2\,\frac{V^2(1-V^2)}{V^2-\lambda^2},$$

and making the obvious substitution

$$w = V^2, \tag{4.4}$$

equation (4.3) becomes

$$8\lambda^2\,\frac{w(1-w)}{w-\lambda^2}\,\varepsilon_{ww} + \frac{2w\left[2\lambda^2(1-w)-(w-\lambda^2)\right]}{w-\lambda^2}\,\varepsilon_w - \frac{1}{2\sin\theta}\frac{\partial}{\partial\theta}\left(\varepsilon_\theta\sin\theta\right) = 0. \tag{4.5}$$

From the definition of λ^2 as $\frac{\gamma-1}{\gamma+1}$, for a real gas $0 < \lambda^2 < 1$.

The partial differential equation (4.4) is elliptic when

$$0 \leq w < \lambda^2$$

and hyperbolic when

$$\lambda^2 < w \leq 1.$$

From (4.4) $w=\lambda^2$ corresponds to a local Mach number of unity and in the field of supersonic flow

$$\lambda^2 < w \leq 1.$$

22. The differential equations of the characteristics of (4.5), which are defined as

$$\pm 4 d\theta = \frac{1}{\lambda}\sqrt{\frac{w-\lambda^2}{1-w}}\,\frac{dw}{w}, \tag{4.6}$$

can be integrated (Ref. 8, p. 192) to yield

$$\theta_1 = \theta \pm \tfrac{1}{4} f(w),$$

where

$$f(w) \equiv \frac{1}{\lambda}\left[\arcsin\frac{2w-(\lambda^2+1)}{\lambda^2-1} - \frac{\pi}{2}\right] + \arcsin\frac{2\lambda^2 w^{-1}-(\lambda^2+1)}{\lambda^2-1} + \frac{\pi}{2}, \tag{4.7}$$

with the initial condition that

$$\theta = \theta_1, \quad w_1 = \lambda^2.$$

By introducing the "characteristic coordinates", defined through

$$\begin{aligned} \xi &= \theta + \tfrac{1}{4} f(w) \\ \eta &= \theta - \tfrac{1}{4} f(w), \end{aligned} \tag{4.8}$$

equation (4.5) is put into the canonical form

$$2\varepsilon_{\xi\eta} - \frac{1}{2\lambda}\,\frac{(2\lambda^2-1)(w-\lambda^2)^2+2\lambda^4(1-\lambda^2)}{(w-\lambda^2)^{3/2}(1-w)^{1/2}}\left(\varepsilon_\xi - \varepsilon_\eta\right) + \frac{\cot\theta}{2}\left(\varepsilon_\xi + \varepsilon_\eta\right) = 0. \tag{4.9}$$

23. From (4.8),

$$\theta = \tfrac{1}{2}(\xi+\eta)$$

$$w = \text{arc } f\{2(\xi-\eta)\},$$

and hence equation (4.9) can be written as

$$2\varepsilon_{\xi\eta} - p(\xi-\eta)(\varepsilon_\xi - \varepsilon_\eta) + q(\xi+\eta)(\varepsilon_\xi + \varepsilon_\eta) = 0. \tag{4.10}$$

With the further substitution

$$x = \xi-\eta, \qquad y = \xi+\eta,$$

from which it is clear that

$$\begin{aligned} x &= \tfrac{1}{2} f(w) \\ y &= 2\theta, \end{aligned} \tag{4.11}$$

equation (4.10) becomes

$$\varepsilon_{xx} - \varepsilon_{yy} + p(x)\,\varepsilon_x - q(y)\,\varepsilon_y = 0, \tag{4.12}$$

with

$$p(x) \equiv \frac{1}{2\lambda}\,\frac{(2\lambda^2-1)(w-\lambda^2)^2 + 2\lambda^4(1-w)}{(w-\lambda^2)^{3/2}(1-w)^{1/2}} \tag{4.13}$$

and

$$q(y) \equiv \tfrac{1}{2}\cot\theta = \tfrac{1}{2}\cot\tfrac{y}{2}. \tag{4.14}$$

The "normal form" of equation (4.12) is obtained by eliminating the first derivatives by use of the substitution

$$\varepsilon(x,y) = E(x,y)\exp\left[-\tfrac{1}{2}\int p(x)\,dx + q(y)\,dy\right], \tag{4.15}$$

resulting in

$$E_{xx} - E_{yy} - \left[\tfrac{1}{2}\{p'(x) + \tfrac{1}{4}p^2(x) - \{\tfrac{1}{2}q'(y) + \tfrac{1}{4}q^2(y)\}\right]E = 0. \tag{4.16}$$

Since p is given explicitly as a function of w, the first of equations (4.11) can be used in writing

$$\int p(x)\,dx = \int p(x)\,\tfrac{1}{2}f'(w)\,dw,$$

and thus

$$\int p(x)\,dx = \frac{1}{4\lambda^2}\int \frac{(2\lambda^2-1)(w-\lambda^2)^2+2\lambda^4(1-\lambda^2)}{w(w-\lambda^2)(1-w)}\,dw,$$

which integrates to

$$\int p(x)\,dx = \ln K_1\, w^{-\frac{1}{4}}(w-\lambda^2)^{\frac{1}{2}}(1-w)^{-(1-3\lambda^2)/4\lambda^2}, \tag{4.17}$$

where K_1 is a constant of the integration which can be taken as unity.

Further,

$$\int q(y)\,dy = \int \cot(y/2)\,d(y/2) = -\ln K_2 \sin(y/2), \tag{4.18}$$

where K_2 is an integration constant which can be given the value one.

With (4.17) and (4.18),

$$\exp\left[-\tfrac{1}{2}\int p(x)\,dx + q(y)\,dy\right] = \sqrt{\sin(y/2)}\; w^{\frac{1}{8}}(w-\lambda^2)^{-\frac{1}{4}}(1-w)^{(1-3\lambda^2)/8\lambda^2}. \tag{4.19}$$

24. Using (4.13) and (4.14) the full form of equation (4.16) is

$$E_{xx} - E_{yy} + \tag{4.20}$$

$$\left[\frac{1}{8}\left(1+\tfrac{1}{2}\cot^2\frac{y}{2}\right) - \frac{\frac{1}{16\lambda^2}\left\{(2\lambda^2-1)(w-\lambda^2)^2+2\lambda^4(1-\lambda^2)\right\}^2 + \frac{1-\lambda^2}{4}w\left\{(2\lambda^2-1)(w-\lambda^2)^2+2\lambda^4(1-\lambda^2)-8\lambda^4(1-w)\right\}}{(w-\lambda^2)^3(1-w)}\right]E = 0.$$

In Fig. 9 the function

$$\frac{1}{8} - \frac{\frac{1}{16\lambda^2}\left\{(2\lambda^2-1)(w-\lambda^2)^2+2\lambda^4(1-\lambda^2)\right\}^2 + \frac{1-\lambda^2}{4}w\left\{(2\lambda^2-1)(w-\lambda^2)^2+2\lambda^4(1-\lambda^2)-8\lambda^4(1-w)\right\}}{(w-\lambda^2)^3(1-w)} \tag{4.21}$$

is plotted as a function of w for $\lambda^2=\frac{1}{6}$ (or $\gamma=1.40$) .

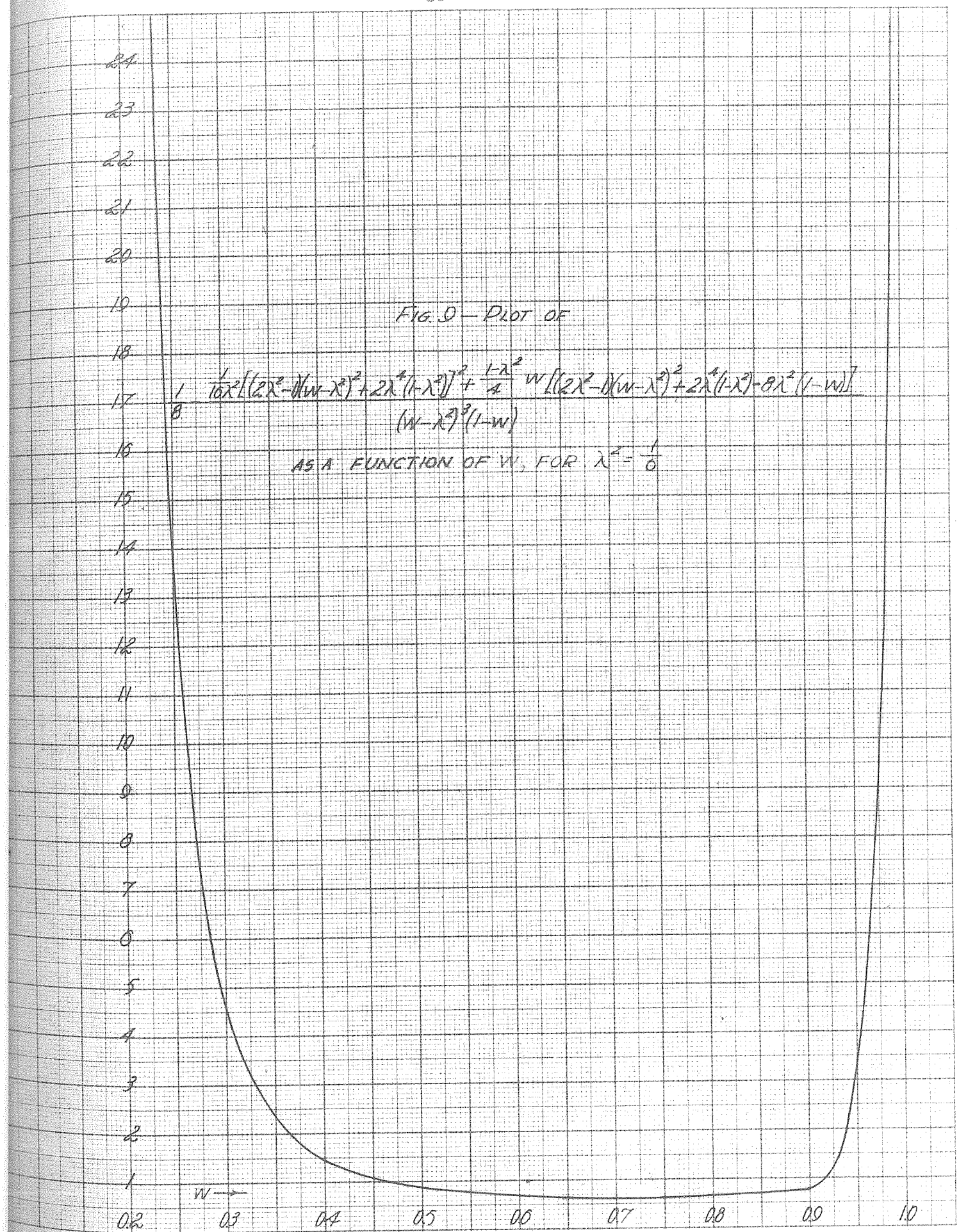

FIG. 9 — PLOT OF

$$\frac{1}{8}\,\frac{\frac{1}{16}\lambda^2[(2\lambda^2-1)(w-\lambda^2)^2+2\lambda^4(1-\lambda^2)]^2+\frac{1-\lambda^2}{4}\,w[(2\lambda^2-1)(w-\lambda^2)^2+2\lambda^4(1-\lambda^2)-8\lambda^2(1-w)]^2}{(w-\lambda^2)^3(1-w)}$$

AS A FUNCTION OF w, FOR $\lambda^2=\frac{1}{10}$

25. For a given value of γ (or λ^2) equation (4.20) can be quite closely approximated to by certain classical equations over a considerable range of values of $M_s(r)$ or $M_s^*(r)$.

The function of (4.21) has a minimum value of about 0.624, and so in the case of the annular wing, for which $\frac{y}{z}$ is close to $\pi/2$, the $\frac{1}{16}\cot^2\frac{y}{z}$ is negligible compared to the other term in the coefficient of E. Then for the annular wing equation (4.20) can be written as

$$E_{xx} - E_{yy} + b^2 E = 0, \tag{4.22}$$

where b^2 may vary considerably in value, as seen from Fig. 9, in passing from the leading to the trailing edge. If b^2 does not vary too greatly, so that it is essentially constant (4.22) becomes the "telegraph equation".

With the ring wing $\frac{y}{z}$ is the angle θ measured from the (z) axis of symmetry and will be small, so that

$$\tfrac{1}{16}\cot^2(y/z) \approx \frac{1}{4y^2},$$

and hence equation (4.20) can be approximated by

$$E_{xx} - E_{yy} + \left[b^2 + \frac{1}{4y^2}\right] E = 0. \tag{4.23}$$

Equation (4.23) can be approximated to by two forms, depending on the size of b^2. When b^2 is small compared to $1/4y^2$, the equation can be written as

$$E_{xx} - E_{yy} + \frac{1}{4y^2} E = -b^2 E, \tag{4.24}$$

and when b^2 is large compared to $1/4y^2$ equation (4.23) is put into

$$E_{xx} - E_{yy} + b^2 E = -\frac{1}{4y^2} E. \tag{4.25}$$

26. Each of the equations (4.24) and (4.25) can be in principle solved by an iteration procedure (Ref. 11); in either case the differential

equation with right hand side zero is first considered -- these have the respective forms

$$E_{xx} - E_{yy} = \frac{1}{4y^2} E = 0 \qquad (4.24)^{(1)}$$

$$E_{xx} - E_{yy} + b^2 E = 0. \qquad (4.25)^{(1)}$$

It will be shown below that it is possible to solve each of $(4.24)^{(1)}$ and $(4.25)^{(1)}$ (which is identical in form with (4.22)) exactly, including the boundary conditions, by an application of the classical Riemann method of integrating hyperbolic linear partial differential equations in two independent variables (see Refs. 12, 13, 14, 15, 16, 17).

The appropriate iteration method will not be detailed here since only the first approximations will be discussed. However, in a complete treatment of the solution by iteration the question of convergence would have to be investigated.

27. Equation $(4.24)^{(1)}$ is valid when b^2 is close to its minimum value, say between 0.7 and 0.624, or for the range

$$0.597 \leq w \leq 0.864.$$

When $\gamma = 1.40$ this corresponds to the case of an airfoil for which the critical Mach numbers at the leading and trailing edges are

$$M_s^*(r_{L.E.}) = 3.58$$

$$M_s^*(r_{T.E.}) = 5.13;$$

for such a wing $M_s^*(r)$ at the trailing edge is 43.3% greater than at the leading edge, which is a significant variation.

In characteristic coordinates equation $(4.24)^{(1)}$ becomes

$$E_{\sigma\tau} + \frac{1/4}{(\tau - \sigma)^2} E = 0,$$

where

$$\sigma = x - y$$

$$\tau = x + y.$$

The Riemann function is a solution of this equation which has the value zero on the two characteristics $\sigma = a$ and $\tau = b$.

By the method detailed in section 50 of Ref. 18 the desired Riemann function U depends upon the variable

$$\zeta \equiv \frac{(\sigma-a)(\tau-b)}{(a-b)(\sigma+\tau)},$$

and satisfies the differential equation

$$\zeta(1-\zeta)U''(\zeta) + (1-2\zeta)U'(\zeta) + \tfrac{1}{4}U(\zeta) = 0.$$

The Riemann function is therefore a hypergeometric function,

$$U(\zeta) = F\left(\tfrac{1+\sqrt{2}}{2}, \tfrac{1-\sqrt{2}}{2}; 1; \zeta\right); \qquad (4.26)_1$$

for negative values of ζ alternative Riemann functions are

$$U(\zeta) = (1-\zeta)^{-\frac{1}{2}(1+\sqrt{2})} F\left(\tfrac{1+\sqrt{2}}{2}, \tfrac{1-\sqrt{2}}{2}; 1; \tfrac{-\zeta}{1-\zeta}\right) \qquad (4.26)_2$$

and

$$U(\zeta) = (1-\zeta)^{-\frac{1}{2}(1-\sqrt{2})} F\left(\tfrac{1+\sqrt{2}}{2}, \tfrac{1-\sqrt{2}}{2}; 1; \tfrac{-\zeta}{1-\zeta}\right). \qquad (4.26)_3$$

For uniform rectilinear flow about slender bodies of revolution the analogous Riemann functions can be identified with the complete elliptic functions of the first and second kinds, but the hypergeometric functions $(4.26)_{1,2,3}$ are not related to any known special functions.

Now that the Riemann function of $(4.24)^{(1)}$ is known the solution in the form of an integral equation can be obtained by use of the general technique detailed in Refs. 12 - 17. However, this solution will not be further pursued, and it will be considered sufficient to

detail the solution of equation (4.22) and to illustrate the procedure by a numerical example.

28. In Appendix I of Ref. 19 the partial differential equation

$$\Phi_{xx}\cos^2\mu - \Phi_{yy}\sin^2\mu + \sigma^2\tan^2\mu\,\Phi = 0 \qquad (4.27)$$

where μ is the Mach angle, is solved by an application of the Riemann method. With $\mu = 45^\circ$ this differential equation becomes formally identical with equations (4.22) and (4.25)[1] when b^2 is a constant, since then (4.27) can be written as

$$\Phi_{xx} - \Phi_{yy} + 2\sigma^2\Phi = 0 \qquad (4.27)'$$

Equation (4.27)' is integrated over a region bounded by the Mach wave leading from the nose of the airfoil, a right running characteristic, and the portion of the upper airfoil surface between the nose and the intersection with the characteristic, as shown in Fig. 10.

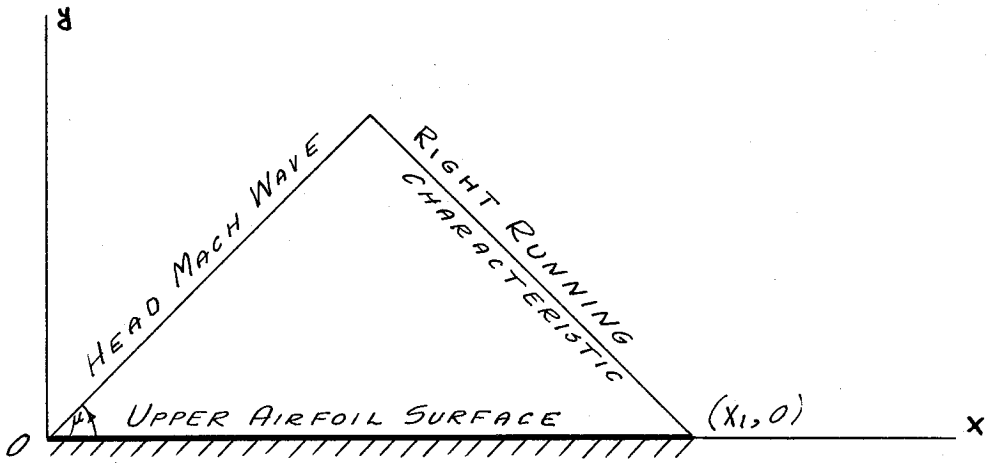

Fig. 10 - Region of Integration of Equation (4.27)' by the Riemann Method

The solution* is shown to be

$$\Phi(x_1, 0) = -\int_0^{x_1} J_0\left[\sqrt{2}\,\sigma(x-x_1)\right]\left(\frac{\partial \Phi}{\partial y}\right)_{y=0} dx \qquad (4.28)$$

where J_0 is the Bessel function of the first kind of order zero and $\left(\frac{\partial \Phi}{\partial y}\right)_{y=0}$ is prescribed along the chord of the airfoil.

This solution can be adapted to the present equations, (4.22) and $(4.25)^{(1)}$, when (4.11) is employed so that those equations take the form

$$E_{\frac{1}{2}f(w)\,\frac{1}{2}f(w)} - E_{2\theta 2\theta} + b^2 E\left\{\tfrac{1}{2}f(w), 2\theta\right\} = 0, \qquad (4.29)$$

where b^2 is constant. The choice of the value of b^2 will be considered in section 30, where a numerical example is exhibited.

The solution of equation (4.29) will be illustrated for the case of the annular wing when b^2 is large compared to $1/4y^2$. It should be noted that in the case of the ring wing, when b^2 is large, the magnitude of the slope of the function (4.21) plotted in Fig. 9 will be very great, and hence if b^2 is to be considered constant the variation in w must be small, implying a wing of very short chord.

29. Equation (4.29) applies to the annular wing when the boundary

---

* If the region of integration of (4.27)' consisted of the lower head Mach wave, a left running characteristic, and the lower surface of the airfoil, the solution would be identical except for a change in sign. Therefore, it is appropriate to write (4.28) as

$$\Phi(x_1, 0) = \mp \int_0^{x_1} J_0\left[\sqrt{2}\,\sigma(x-x_1)\right]\left(\frac{\partial \Phi}{\partial y}\right)_{y=0} dx, \qquad (4.28)'$$

where the (-) and (+) signs apply respectively to the upper and lower surfaces of the airfoil. This approximation must thus neglect differences (except for sign) in the perturbations on the top and bottom of the airfoil.

condition of tangent surface flow is imposed on the plane r rather than directly on the wing, as in Fig. 11 below.

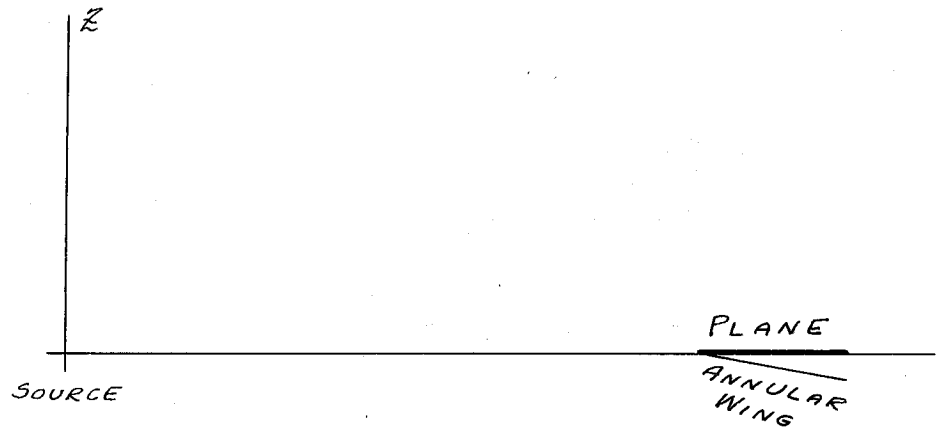

Fig. 11 - For the Annular Wing the Boundary Condition of Tangent Surface Flow is Applied on the Plane to which the Wing Approximates

Then the analog of $\left(\frac{\partial \Phi}{\partial y}\right)_{y=0}$ in (4.28) is $\left(\frac{\partial E}{\partial(\epsilon\theta)}\right)_{\theta=\pi/\epsilon}$, which first must be expressed as a function of $\mathcal{E}_\theta(r,\theta)$, the actual boundary condition on the airfoil. For the annular wing $g(y)$ in (4.15) may be approximated by zero. Then, through the relation (4.15) between $\mathcal{E}(r,\theta)$ and $\left[E\ \frac{1}{\epsilon}f(w), \epsilon\theta\right]$, the boundary condition on the wing has the form

$$E^*_{\epsilon\theta}\left[\tfrac{1}{\epsilon}f(w), \pi\right] = -\frac{\alpha}{\epsilon\lambda}\,\gamma\, w^{3/8}(w-\lambda^2)^{1/4}(1-w)^{-(1-3\lambda^2)/8\lambda^2} \qquad (4.30)$$

where α is the approximately constant angle of attack, and $E^* \equiv E/a_*$ is the analog of $M^*(r,\theta)$ as defined in section 18.

In the neighborhood of the sonic line the linearized theory is not valid, and so the leading edge must be sufficiently far removed from $w=\lambda^2$, at which the function f vanishes. By placing the leading edge at $\lambda^2 < w_{L.E.} < 1$, for which $f(w_{L.E.}) \neq 0$, the perturbation vanishes up to this point and formula (4.28)' becomes

$$E^*\left\{\tfrac{1}{2}f(w_1),\pi\right\} = \pm\frac{\alpha}{2\lambda}\int_{\frac{1}{2}f(w_{L.E.})}^{\frac{1}{2}f(w_1)} r w^{3/8}(w-\lambda^2)^{1/4}(1-w)^{-(1-3\lambda^2)/8\lambda^2} J_0\left[b\left\{\tfrac{1}{2}f(w)-\tfrac{1}{2}f(w_1)\right\}\right] d\tfrac{1}{2}f(w) \quad (4.31)$$

where now the (+) and (-) signs apply to the upper and lower surfaces, respectively.

In formulas (3.8) and (3.13) the critical Mach number M^* of the perturbed flow and the pressure coefficient were shown to be dependent only upon the ratio of the radial component of the perturbation in the source flow critical Mach number to the source flow critical Mach number. Therefore, it is desirable to compute the value of $m_r^*/M_s^*(r_1)$ along the airfoil surface. The relation between this quantity and $E^*\left\{\frac{1}{2}f(w_1),\pi\right\}$ is readily seen to be

$$\frac{m_r^*}{M_s^*(r_1)} = \lambda w_1^{-\frac{1}{8}}(w_1-\lambda^2)^{\frac{1}{4}}(1-w_1)^{\frac{1-7\lambda^2}{8\lambda^2}}\left[E^*_{\frac{1}{2}f(w_1)}\left\{\tfrac{1}{2}f(w_1),\pi\right\} - \frac{p(x)}{2}E^*\left\{\tfrac{1}{2}f(w_1),\pi\right\}\right]\frac{dM_s^*(r)}{dr}, \quad (4.32)$$

where $p(x)$ is defined in (4.13). From equation (2.9)

$$\frac{dM_s^*(r)}{dr} = \frac{2}{A}\,\frac{M_s^{*3/2}(r)\left[1-\lambda^2 M_s^{*2}(r)\right]^{(2\gamma-1)/2(\gamma-1)}}{M_s^{*2}(r)-1}$$

$$= \frac{2\lambda^{1/2}}{A}\,\frac{w^{3/4}(1-w)^{(2\gamma-1)/2(\gamma-1)}}{w-\lambda^2},$$

using (4.4). Further, by Leibniz's formula, $E^*_{\frac{1}{2}f(w_1)}$ is given from (4.32) as

$$E^*_{\frac{1}{2}f(w_1)}\left\{\tfrac{1}{2}f(w_1),\pi\right\} = \pm\frac{\alpha}{2\lambda}\left[r_1 w_1^{\frac{3}{8}}(w_1-\lambda^2)^{\frac{1}{4}}(1-w_1)^{-\frac{1-3\lambda^2}{8\lambda^2}} + b\int_{\frac{1}{2}f(w_{L.E.})}^{\frac{1}{2}f(w_1)} r w^{\frac{3}{8}}(w-\lambda^2)^{\frac{1}{4}}(1-w)^{-\frac{1-3\lambda^2}{8\lambda^2}} J_1\left[b\left\{\tfrac{1}{2}f(w)-\tfrac{1}{2}f(w_1)\right\}\right] d\tfrac{1}{2}f(w)\right].$$

Thus, the quantity to be computed is given by

$$\frac{m_r^*}{M_s^*(r_1)} = \pm\frac{\alpha\lambda^{1/2}}{A}\,\frac{(1-w_1)^{\frac{\gamma+2}{4(\gamma-1)}}}{w_1^{1/8}(w_1-\lambda^2)^{3/4}}\left[bI_1(w_1) - P(w_1)I_0(w_1) + r_1 w_1^{3/8}(w_1-\lambda^2)^{1/4}(1-w_1)^{-\frac{1-3\lambda^2}{8\lambda^2}}\right], \quad (4.33)$$

where

$$P(w) \equiv p(x), \text{ where } x = \tfrac{1}{2} f(w),$$

$$I_0(x) \equiv \int_{\frac{1}{2}f(w_{L.E.})}^{\frac{1}{2}f(w_1)} r\, w^{3/8} (w-\lambda^2)^{1/4} (1-w)^{-\frac{1-3\lambda^2}{8\lambda^2}} J_0\left[b\left\{\tfrac{1}{2}f(w) - \tfrac{1}{2}f(w_1)\right\}\right] d\tfrac{1}{2}f(w),$$

$$I_1(w_1) \equiv \int_{\frac{1}{2}f(w_{L.E.})}^{\frac{1}{2}f(w_1)} r\, w^{3/8} (w-\lambda^2)^{1/4} (1-w)^{-\frac{1-3\lambda^2}{8\lambda^2}} J_1\left[b\left\{\tfrac{1}{2}f(w) - \tfrac{1}{2}f(w_1)\right\}\right] d\tfrac{1}{2}f(w).$$

30. As a numerical example* the values of M^* and c_{p_s} will be computed from formula (4.31) for a zero thickness annular wing which has its leading and trailing edges on spherical surfaces 60 and 70 units, respectively, from the supersonic source. At the leading edge the local Mach number is assumed to be

$$M_s(r_{L.E.}) = \sqrt{2}$$

and γ is chosen to have the value 1.40**; then, from equation (2.10),

$$M_s^*(r_{L.E.}) = 1.309.$$

With this pair of values of r and $M_s^*(r)$ the value of A is computed from equation (2.9)a to be 45.083. At the trailing edge the local and critical Mach numbers are

---

* The same numerical data used in this example are employed later (section 42), in an illustration of the use of the Method of Characteristics (see Chapter V) since it will be of interest to compare the results given by these two distinct methods.

** Since the theory is a linear one the particular value of γ is not of predominant importance and in a numerical example its size can be based on convenience; 1.40 is chosen so that certain published tables, which are computed for only this value of γ, can be used.

$$M_s(r_{T.E.}) = 1.876$$

$$M_s^*(r_{T.E.}) = 1.574,$$

or 32.6 and 20.2 percent, respectively, greater than their values at the leading edge, showing that there is a significant variation in Mach number over the wing.

The annular wing will be assumed to have the form of the lateral surface of a truncated right circular cone with a semi-vertex angle of of 84°, having its leading edge in the x,y plane. At a given point on the wing the angle of attack α will be the angle between the x,y plane and the streamline to the point (see Fig. 12), and will vary between 6° at the leading edge and 5°9' at the trailing edge; however, within the

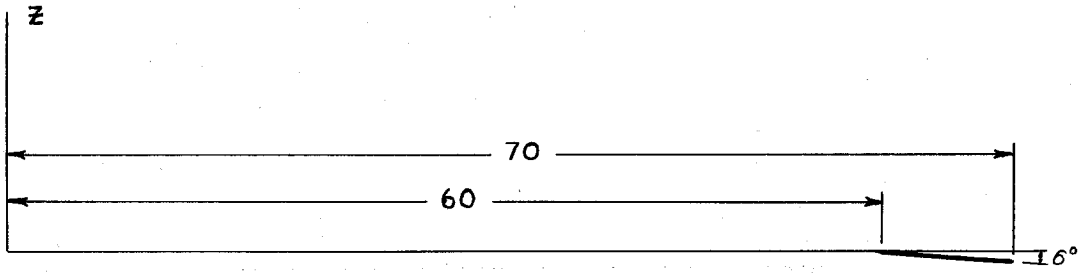

Fig. 12 - Trace of the Annular Wing of the Numerical Example

frame of the linearized theory α can be considered constant and equal to some value along the airfoil chord. In this example α will be 6°, the value at the leading edge. Further, at the leading edge

$$f(w_{L.E.}) = -0.3272,$$

and at the trailing edge

$$f(w_{T.E.}) = -0.8026.$$

From Fig. 9, when $r=60$ the coefficient b of E in equation (4.23) has the value 2.392; and when $r=70$, $b=1.156$. For points w_1 on the

airfoil close to the leading edge the maximum values of the arguments of J_0 will be very small, and so J_0 will be essentially unity, irrespective of the value assigned to b. Hence, one might expect the best overall results to be obtained for a value of b which corresponds to a point somewhere between the leading and trailing edges. To gain some idea of the influence of b on $m_r^*/M_s^*(r)$, the computations were carried out for four values of b, corresponding to

1) $b = 0$

2) $b = 2.392$, at the leading edge,

3) $b = 1.429$, at the mid-chord,

4) $b = 1.156$, at the trailing edge.

The integrals $I_0(w_1)$ and $I_1(w_1)$ of (4.33) were computed by Simpson's one-third rule for eleven stations spaced equidistantly along the chord, starting at the leading edge. In Fig. 13 the functions $P(w_1)$, $(1-w_1)^{2.125}/w_1^{1/8}(w_1-1/6)^{3/4}$, $r_1 w_1^{3/8}(w_1-1/6)^{1/4}/(1-w_1)^{3/8}$, and the integrals $I_0(w_1)$ and $I_1(w_1)$ are plotted as functions of the distance r_1 from the source along the airfoil chord. With these curves the computation of $m_r^*/M_s^*(r)$ is direct and leads to a set of curves, for the different values of b, showing that expression as a function of r_1, as in Fig. 14. From that figure it is clear that for this particular example the results are only slightly influenced by the value (0 - 2.392) assigned to b.

Figure 14 also contains the value of $m_r^*/M_s^*(r)$ computed by the Method of Characteristics for this same annular wing. The Method of Characteristics must be considered as a standard for comparison, since its accuracy can be indefinitely improved by iteration. From the

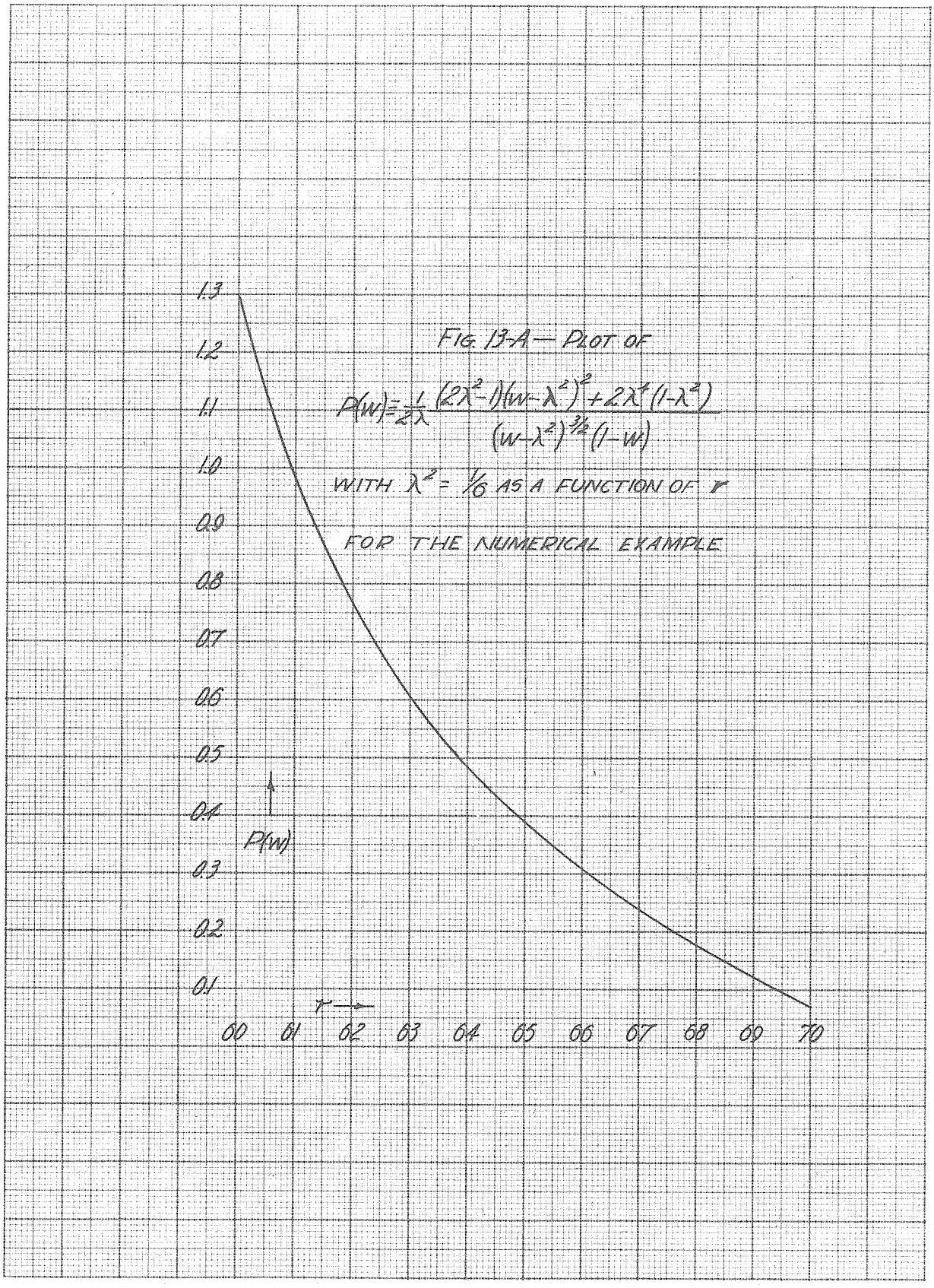

FIG. 13-A — PLOT OF

$$P(w) = \frac{1}{2\lambda} \frac{(2\lambda^2 - 1)(w - \lambda^2)^{\frac{1}{2}} + 2\lambda^4 (1 - \lambda^2)}{(w - \lambda^2)^{\frac{3}{2}} (1 - w)}$$

WITH $\lambda^2 = 1/6$ AS A FUNCTION OF r

FOR THE NUMERICAL EXAMPLE

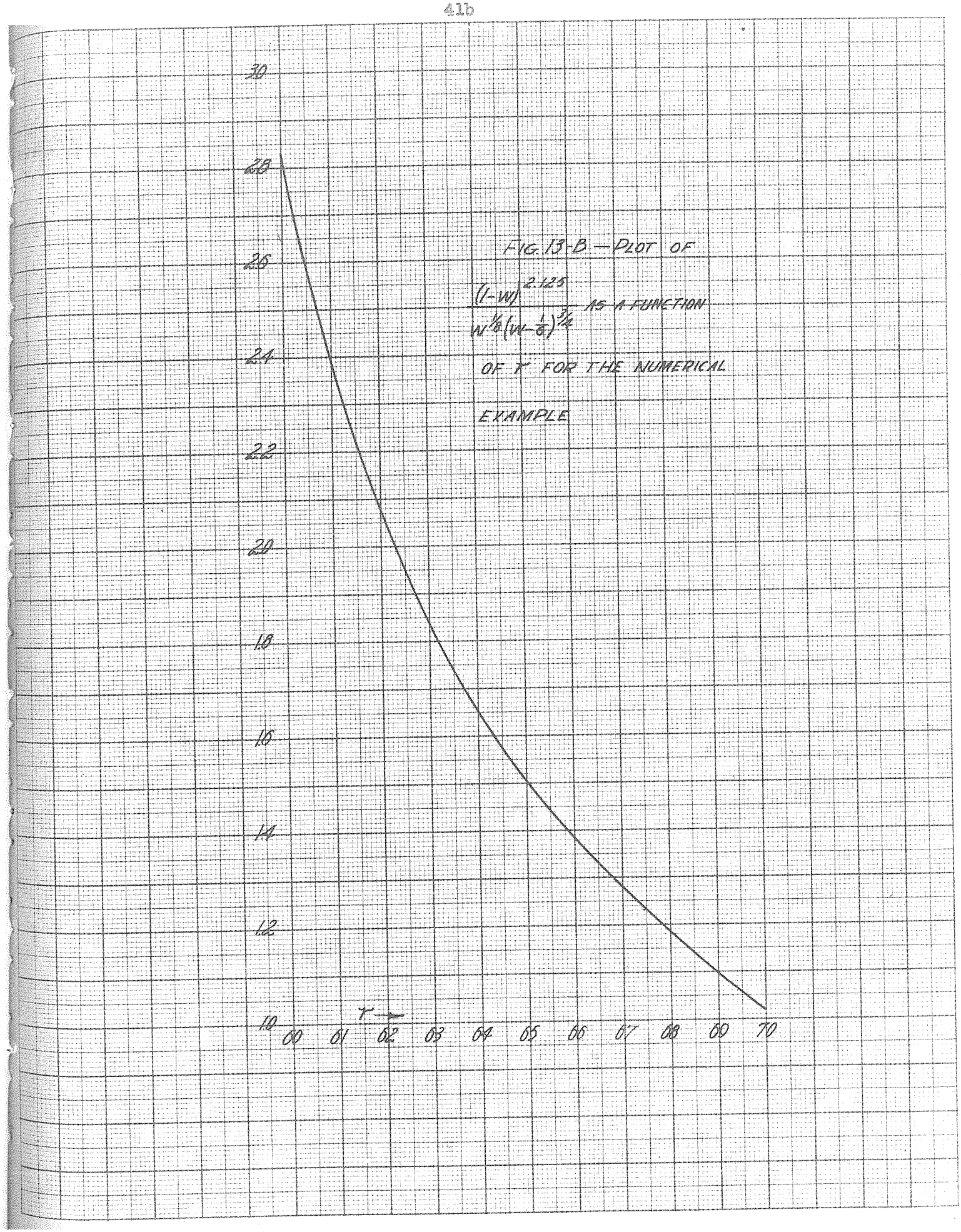

FIG. 13-B — PLOT OF $\frac{(1-W)^{2.125}}{W^{1/8}(W-\frac{1}{8})^{3/4}}$ AS A FUNCTION OF τ FOR THE NUMERICAL EXAMPLE

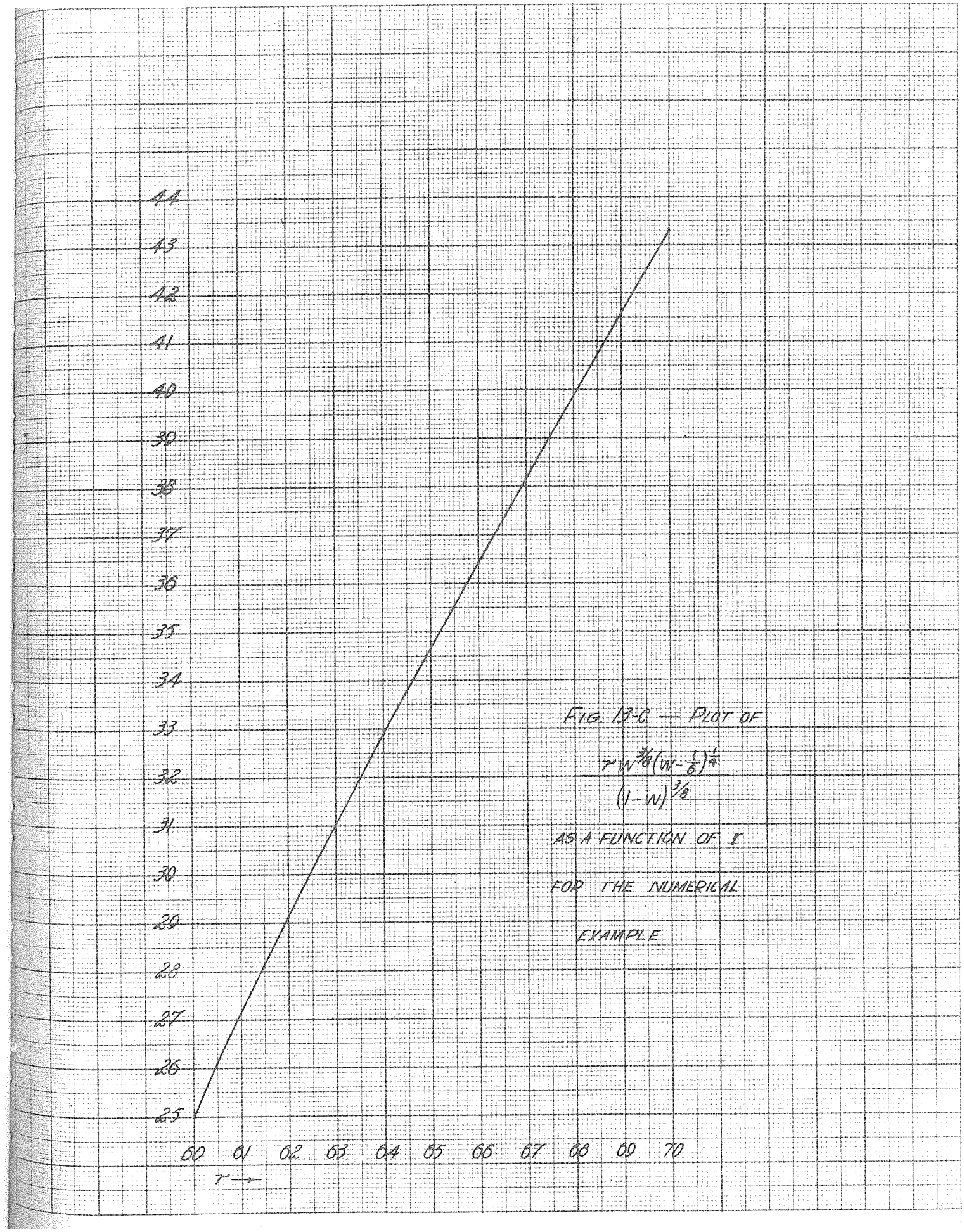

FIG. 13-C — PLOT OF

$$\frac{r\,W^{3/8}(W-\frac{1}{6})^{\frac{1}{4}}}{(1-W)^{3/8}}$$

AS A FUNCTION OF r

FOR THE NUMERICAL

EXAMPLE

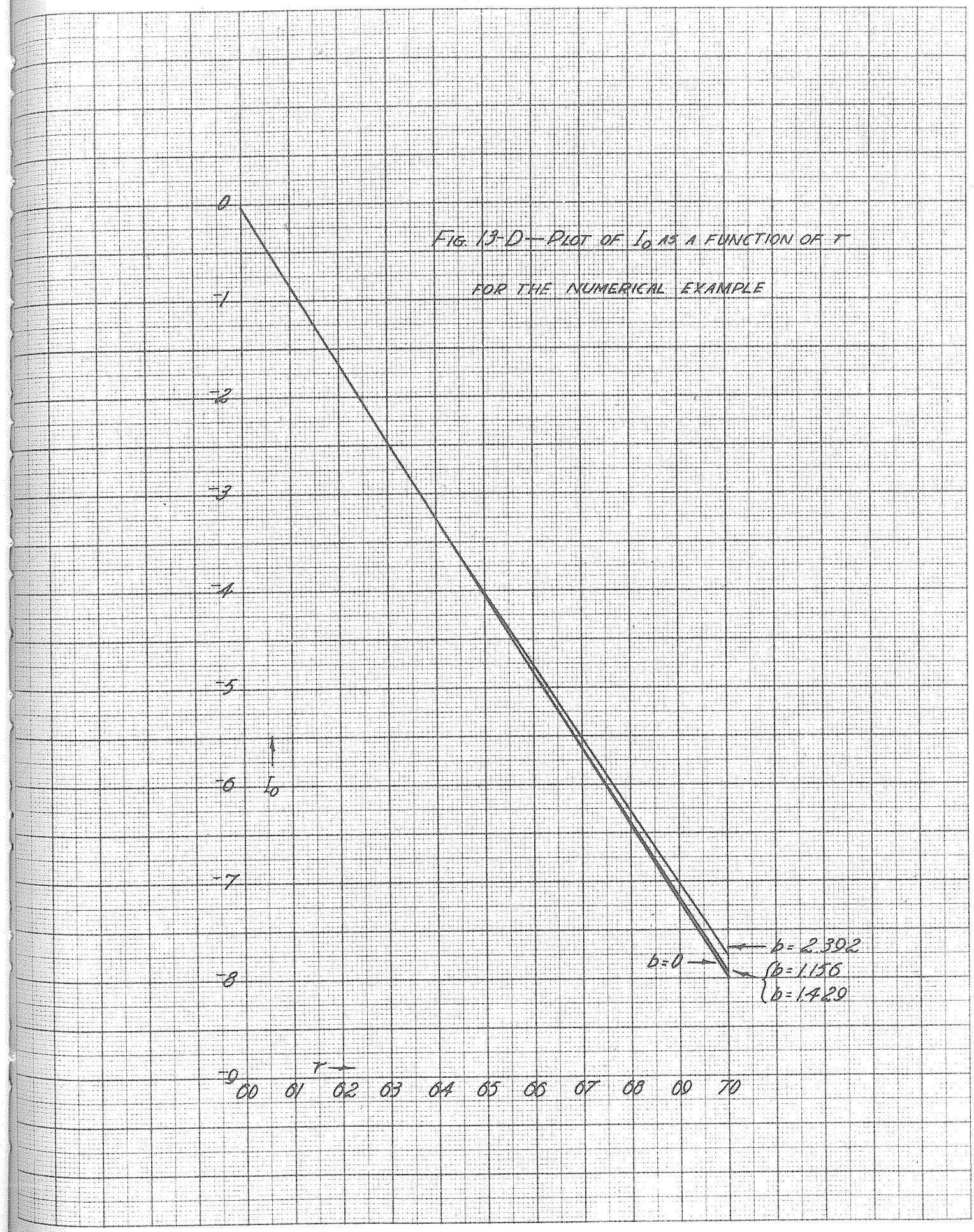

FIG. 13-D — PLOT OF I_0 AS A FUNCTION OF τ FOR THE NUMERICAL EXAMPLE

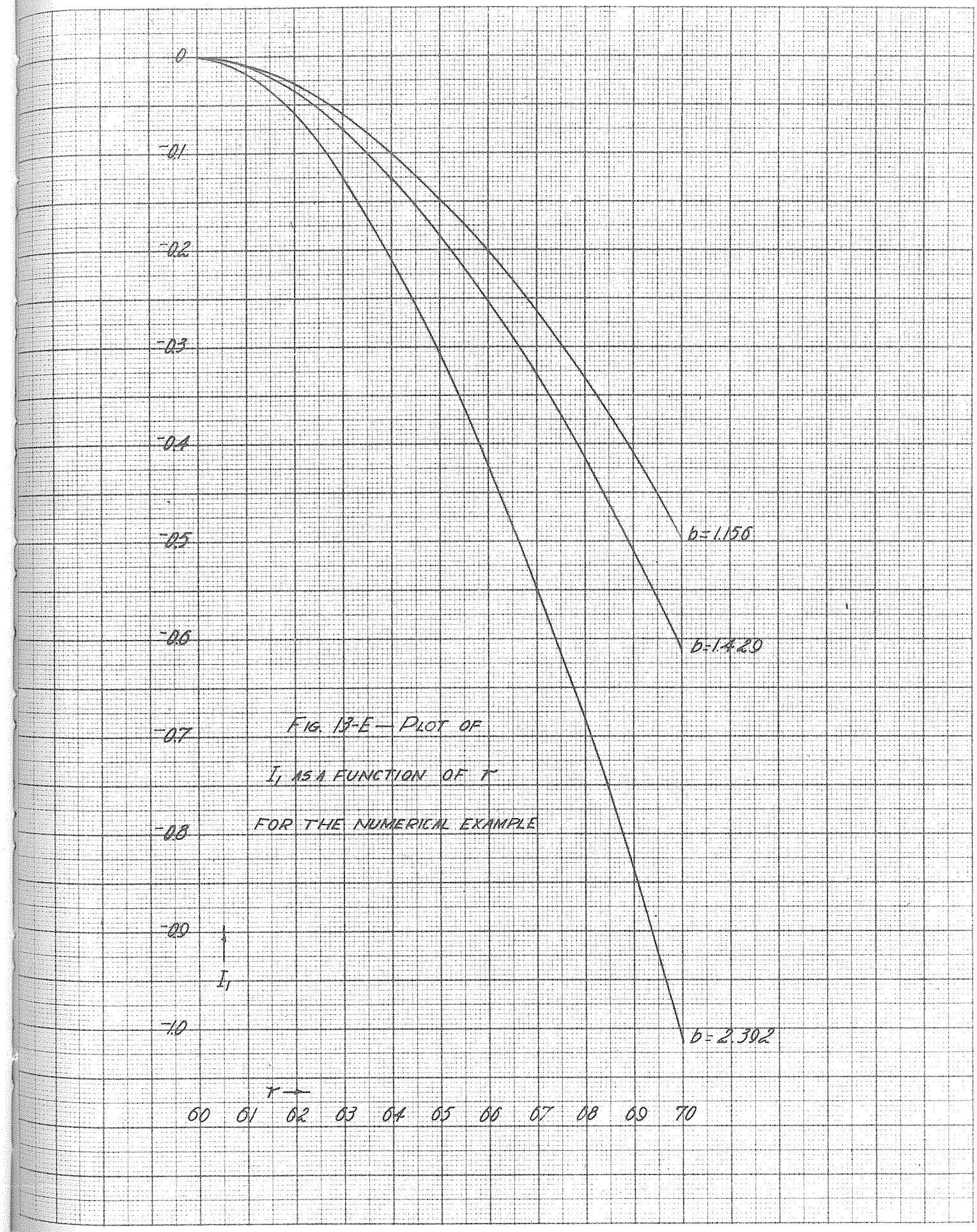

FIG. 13-E — PLOT OF I_1 AS A FUNCTION OF τ FOR THE NUMERICAL EXAMPLE

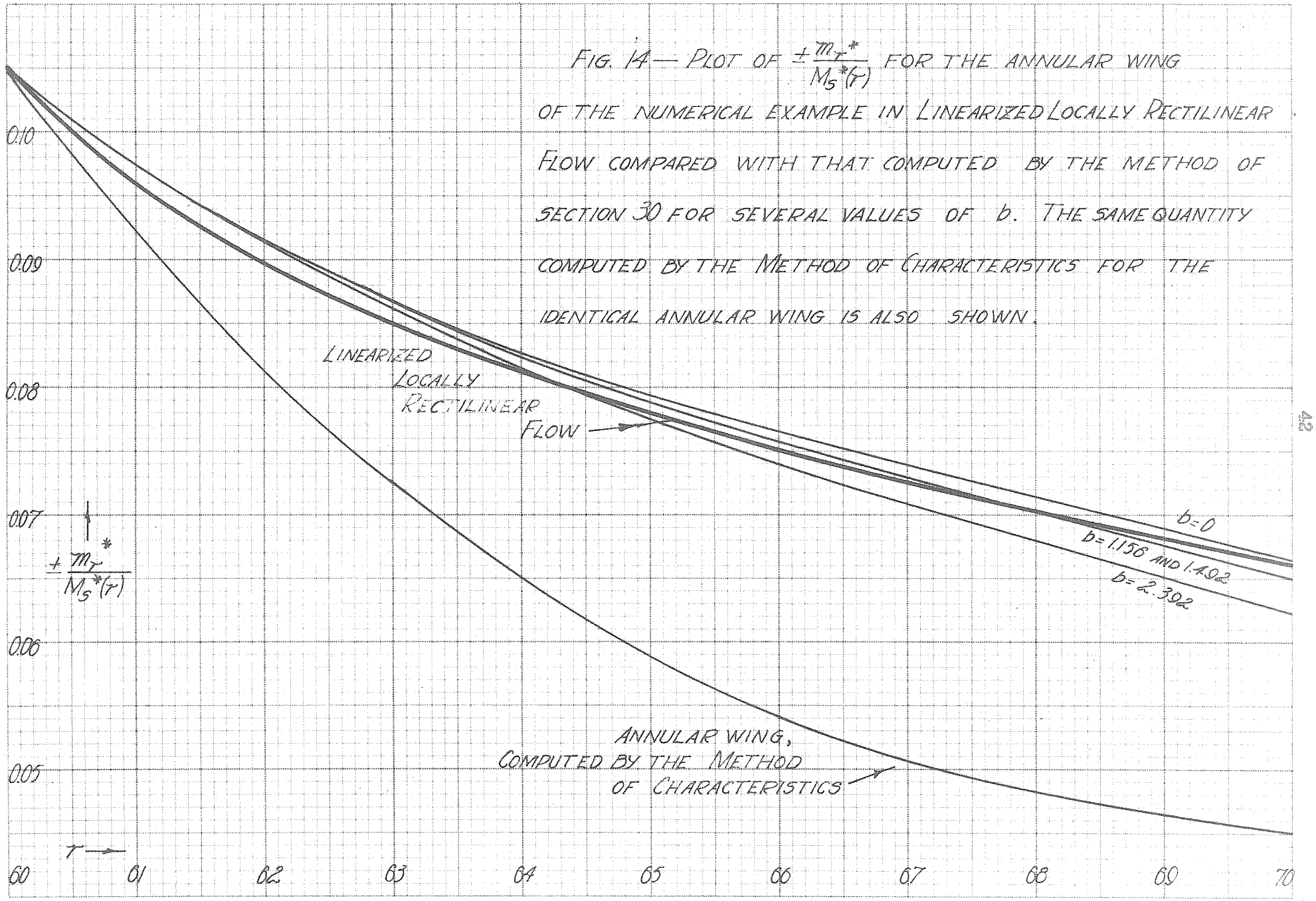

FIG. 14 — PLOT OF $\pm \frac{m_T^*}{M_S^*(\tau)}$ FOR THE ANNULAR WING OF THE NUMERICAL EXAMPLE IN LINEARIZED LOCALLY RECTILINEAR FLOW COMPARED WITH THAT COMPUTED BY THE METHOD OF SECTION 30 FOR SEVERAL VALUES OF b. THE SAME QUANTITY COMPUTED BY THE METHOD OF CHARACTERISTICS FOR THE IDENTICAL ANNULAR WING IS ALSO SHOWN.

comparison it can be seen that the numerical procedure detailed in this chapter does not give results which agree too well with those obtained by the Method of Characteristics. However, the results of this section are very close to those computed for a wing in linearized locally rectilinear flow, which is not surprising, since when $b=0$ equation (4.22) becomes the two dimensional wave equation, which governs linearized rectilinear flow, and it has been shown that a value of $0 \leq b \leq 2.392$ is at most a secondary influence on the solution. Hence, it appears that formula (4.33), which gives a very good approximation to the results for linearized locally rectilinear flow, is not of much practical value (at least for the numerical example of this section), since formulas (3.13) and (3.14) will give the same answers in about one per cent of the time and effort.

V. SOLUTION OF THE PERTURBATION POTENTIAL EQUATION BY THE METHOD OF CHARACTERISTICS

31. The Method of Characteristics was originated in 1929 by Prandtl and Busemann (Refs. 21, 22) to solve problems in plane, steady, supersonic potential flows. In recent years the ideas have been extended by numerous authors (Refs. 23 - 26) to axially symmetric space flows and even to fully three dimensional motions about bodies of revolution at small angles of attack (Ref. 6).

As usually employed in the approximate solution of the hyperbolic partial differential equations of supersonic flow theory, the Method of Characteristics is in principle a numerical, graphical, or numerical and graphical, equivalent of Monge's method of solving such equations. This affinity is highly significant, because for the solution of second order "quasi-linear"* partial differential equations one of the most important general analytical procedures is that due to the French geometer; hence the Method of Characteristics will provide a highly general approximate solution.

32. Monge's method is applied to the important class of equations with the generic form

$$R(x,y,z,z_x,z_y)\,z_{xx} + S(x,y,z,z_x,z_y)\,z_{xy} + T(x,y,z,z_x,z_y)\,z_{yy} - V(x,y,z,z_x,z_y) = 0, \quad (5.1)$$

where x,y are the independent variables, and $z(x,y)$ is the dependent variable.

---

* Linear in the highest order derivatives.

Now, most of the well known methods of attacking partial differential equations of the form (5.1) aim to discover the functional relation

$$\zeta(x,y,z)=0, \quad \frac{\partial \zeta}{\partial z} \neq 0, \tag{5.2}$$

which identically satisfies the equation. Monge's suggested procedure, however, is not designed to produce directly the solution (5.2) of (5.1), but instead undertakes to discover a pair of intermediate integrals, of the form

$$\begin{aligned} f_1(x,y,z,z_x,z_y)&=0 \\ f_2(x,y,z,z_x,z_y)&=0, \end{aligned} \tag{5.3}$$

each satisfying the differential equation (5.1). In principle, the two intermediate integrals $f_1=0$ and $f_2=0$ may be considered as a pair of simultaneous equations in z_x and z_y and solved to give

$$\begin{aligned} z_x &= z_x(x,y,z) \\ z_y &= z_y(x,y,z). \end{aligned} \tag{5.4}$$

It is just because Monge's method applied to equation (5.1) leads to the relations (5.4), and does not waste itself in a direct effort to solve that very difficult equation, that it is a valuable procedure for the solution of the supersonic potential flow equations. For, in the problems of gas dynamics the wanted quantities are usually the velocities, the first order derivatives of the dependent variable, which is exactly what the Monge method provides.

The first phase of Monge's procedure requires the concommitant solution of the equations "subsidiary" to (5.1):

$$Rdy^2 - Sdxdy + Tdy^2 = 0 \tag{5.5}$$

$$\rho\, dz_x\, dy + T\, d\varepsilon_y\, dx - V\, dx\, dy = 0 \tag{5.6}$$

In texts on Partial Differential Equations (section 76, Ref. 27) equation (5.1) is shown to be satisfied by any functional relation simultaneously satisfying (5.5) and (5.6). Equation (5.5) represents, in differential form, the characteristics of the parent equation (5.1).

33. In the supersonic region of the compressible source flow the differential equations of the Mach lines are given as

$$\frac{r\, d\theta}{dr} = \pm \frac{1}{\sqrt{M_s^2(r) - 1}}. \tag{5.7}$$

For, moving from one point P_1 to its neighbor P_2 along a segment of a Mach line which is short enough to be considered straight (Fig. 15),

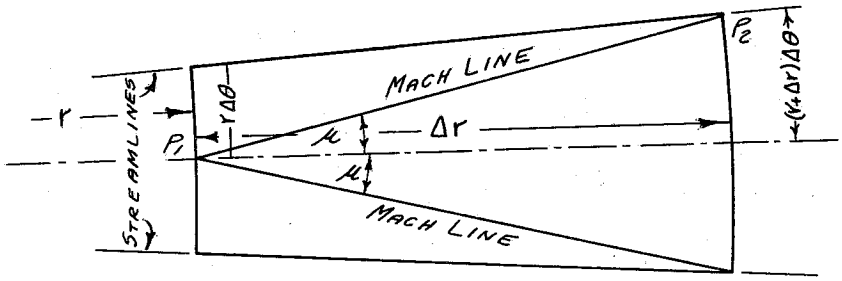

Fig. 15

the relation between the changes Δr and $\Delta\theta$ in the coordinates r and θ is seen to be

$$\frac{(r+\Delta r)\Delta\theta}{\Delta r} = \pm \tan \mu .$$

In the limit, as Δr and $\Delta\theta$ approach zero,

$$\frac{r\, d\theta}{dr} = \pm \tan \mu , \tag{5.8}$$

where

$$\mu = \sin^{-1} \frac{1}{M_s(r)} = \tan^{-1} \frac{1}{\sqrt{M_s^2(r) - 1}} ; \tag{5.9}$$

combining (5.8) and (5.9) gives the differential equation (5.7) of the Mach lines.

Equation (3.6) will now be solved by the Method of Characteristics. For this purpose it is convenient to write the differential equation in the form

$$r^2\left[M_s^2(r)-1\right]\varepsilon_{rr} - \varepsilon_{\theta\theta} + 2r\,\frac{(\gamma-1)\,M_s^4(r) + M_s^2(r) + 1}{M_s^2(r)-1}\,\varepsilon_r - \nu\cot\theta\,\varepsilon_\theta = 0, \qquad (3.6)'$$

where $\nu=1$ for the ring wing; and the equation representing the annular wing, for which $\theta \simeq \pi/2$, is approximated by choosing $\nu=0$. The differential equations of the characteristics are

$$\frac{r\,d\theta}{dr} = \pm\frac{1}{\sqrt{M_s^2(r)-1}}\,; \qquad (5.7)'$$

the "left running" characteristic has the positive sign and the "right running" characteristic has the negative sign.

Comparing (5.7) with (5.7)' it is clear that the differential equations of the characteristics of the linearized perturbation potential equation (3.6) are the same as the differential equations of the Mach lines in the source flow. Since the characteristics of (3.6) are also the Mach lines in the flow, and conversely, the characteristics in the deranged source flow will be identical with the characteristics of the undisturbed flow. That is, the characteristics of the equation (3.6) to which the solution is sought are precisely the known characteristics (Mach lines) of the known source flow.

34. The characteristics can be readily constructed, since the Mach number $M_s(r)$ of the source flow is known from (2.9) as a function of r and $M_s^*(r)$ is known as a function of $M_s(r)$ from (2.11). The constant

A is fixed in size by prescribing an initial condition: a value of $M_s(r)>1$ $(\text{or } \mu<\frac{\pi}{2})$ corresponding to an arbitrarily assigned value of r. That is, the initial condition is imposed on a spherical surface centered at the source, on which the Mach number $M_s(r)$ is constant; in a plane of symmetry the trace of the spherical surface is a circular arc. On this sphere (or circular arc) the streamlines are radial.

Since the source flow is completely known, that part of the field described by the source potential has no interest here, and so the initial conditions are chosen as far downstream as possible, on the spherical surface passing through the leading edge of the wing. Except at the leading edge the flow downstream of this surface is for some distance undisturbed; then it enters the zone of action, in which are confined the disturbances due to the wing (so the initial condition is really applied at only the nose of the wing). The region of influence of the wing is the only one of interest here, and all computations will begin at the leading edge.

For the purpose of actually constructing the characteristics defined by (5.7) the set of curves in Fig. 16 is convenient and accurate.

35. When applied to (3.6) the second of Monge's equations, (5.6), is

$$r^2\left[M_s^2(r)-1\right]d\theta\, d\varepsilon_r - dr\, d\varepsilon_\theta + \left[2r\frac{(\gamma-1)M_s^4(r)+M_s^2(r)+1}{M_s^2(r)-1}\varepsilon_r - \nu\cot\theta\,\varepsilon_\theta\right]dr\,d\theta=0, \quad (5.10)$$

a differential relation between ε_r and ε_θ, the first derivatives of the perturbation potential $\varepsilon(r,\theta)$, at every point of the flow field. Dividing (5.10) by dr, associating $d\theta$ and dr by way of the relation (5.7), which holds only along the characteristics, and finally

$$\alpha = \alpha(r) = \text{arc}\ \sin \frac{1}{M_s(r)}$$

$$\left(\frac{r}{A}\right)_{air} = M_s^{*\frac{1}{2}}(r)\left[1 - \frac{1}{6}M_s^{*2}(r)\right]^{-1.25}$$

$$M_s^{*2}(r) = \frac{1.2\,M_s^2(r)}{1+0.2\,M_s^2(r)}$$

EXAMPLE OF THE USE OF THESE CURVES:

ASSUME $\frac{r}{A} = 1.39$, DETERMINE $M_s^*(1.39) = 1.406$

LOCATE $M_s = 1.568$ FOR $M_s^* = 1.406$, AND

FINALLY OBTAIN $\alpha = 38°46'$ WHEN $M_s = 1.568$

$M_s^*(r)$ — α

$M_s(r) \longrightarrow$ 1.4 1.5 1.6 1.7 1.8 1.9 2.0

$\frac{r}{A} \longrightarrow$ 1.36 1.38 1.40 1.42 1.44 1.46 1.48 1.50 1.52 1.54 1.58 1.60

1.66 1.64 1.62 1.60 1.58 1.56 1.54 1.52 1.50 1.48 1.46 1.44 1.42 1.40 1.38 1.36 1.34

45° 44° 43° 42° 41° 40° 39° 38° 37° 36° 35° 34° 33°

FIG. 16

CURVES EMPLOYED IN THE CONSTRUCTION OF THE CHARACTERISTICS OF THE SUPERSONIC SOURCE FLOW

multiplying by $\frac{1}{r\sqrt{M_s^2(r)-1}}$, there results

$$\pm d\varepsilon_r - \frac{1}{r\sqrt{M_s^2(r)-1}}\, d\varepsilon_\theta + 2\left[\frac{(\gamma-1)M_s^4(r)+M_s^2(r)+1}{M_s^2(r)-1}\,\varepsilon_r - \nu\frac{\cot\theta}{r\sqrt{M_s^2(r)-1}}\,\varepsilon_\theta\right] d\theta = 0. \qquad (5.11)$$

For economy in writing set

$$S(r) \equiv \frac{1}{r\sqrt{M_s^2(r)-1}} \qquad (5.12)$$

$$R(r) \equiv 2\,\frac{(\gamma-1)M_s^4(r)+M_s^2(r)+1}{M_s^2(r)-1}. \qquad (5.13)$$

With these abbreviations (5.11) becomes

$$\pm d\varepsilon_r - S(r)\, d\varepsilon_\theta + \left[R(r)\,\varepsilon_r - \nu\, S(r)\cot\theta\,\varepsilon_\theta\right] d\theta = 0, \qquad (5.14)$$

the so called "compatibility equations," each representing in differential form a first integral of (3.6) along its characteristics. Dividing (5.14) by $a_*(\neq 0)$ leads to a form of the compatibility equations in which m_r^* and m_θ^* are employed:

$$\pm dm_r^* - S(r)\, d(r m_\theta^*) + \left[R(r)\, m_r^* - \nu\,\beta^{-1}(r)\cot\theta\, m_\theta^*\right] d\theta = 0, \qquad (5.14)'$$

where

$$\beta^{-1}(r) = r\,S(r) = \frac{1}{\sqrt{M_s^2(r)-1}}. \qquad (5.15)$$

A straightforward attempt at an exact integration of equations (5.14)' must fail because the variation of m_r^* and m_θ^* with r and θ is not known. However, these difficulties are resolved if exact techniques are abandoned and the continuous web of characteristics is approximated to by a finite member of polygonal curves across which the fluid properties suffer finite, though small, changes. The differential equations (5.14)' are thus replaced by difference equations, each integrated stepwise along one set of characteristics.

Because of the approximate nature of the calculations the fluid

properties are known at only a set of isolated points, the intersections of the two families of characteristics.

36. It is now assumed that the characteristics of equation (3.6), defined by (5.7), have been constructed in the form of a network of lines, with the leading edge of a wing at a nodal point. Since the ring- and annular airfoils have been assumed to be the only disturbing influences which cause a small axially symmetric derangement of a supersonic source flow, one or the other of these wings can be the only solid boundary in the flow, except for possible walls to contain the fluid. Unless otherwise noted, the analysis to follow applies equally to the ring- and annular-wings.

The two characteristics which intersect at the leading edge will be termed the "head characteristics" or "head waves". Upstream of the head waves the fluid motion is a pure supersonic source flow, so attention is confined to the downstream region, in which the fluid disturbed by the wing is contained (see Fig. 17 for a representation of the characteristic net above the surface of a wing; the lower net is similar).

37. The two simultaneous equations (5.14)' are now integrated step by step, starting with the assumed known flow conditions at the two nodal points U(upper) and L(lower), not on the same characteristic, the object being to determine the values of m_r^* and m_θ^* at the point of intersection (1) of the right-running characteristic through U and the left-running characteristic through L.

On the right running characteristic the negative sign in (5.14)' applies, and integrating from U to 1 there results

$$-\int_U^1 dm_r^* - \int_U^1 S(r)\, d(r m_\theta^*) + \int_U^1 \left[R(r) m_r^* - \nu \beta^{-1}(r) \cot\theta\, m_\theta^*\right] d\theta = 0. \qquad (5.15)R$$

Similarly, integrating along the left running characteristic from L to 1,

$$+\int_L^1 dm_r^* - \int_L^1 S(r)\, d(r m_\theta^*) + \int_L^1 \left[R(r) m_r^* - \nu \beta^{-1}(r) \cot\theta\, m_\theta^*\right] d\theta = 0. \qquad (5.15)L$$

Since the small wing is a solid boundary in a supersonic stream the flow over the upper surface is not influenced by the fluid moving over the lower surface. Hence the computations in the characteristic nets above and below the wing may be carried out independently of one another.

For convenience, in computing m_r^* and m_θ^* at points (1) in the perturbed flow the computations are separated into six classifications, according as the points (1) are

a) Boundary points: on the upper surface of the wing,

b) Semi-interior points: on the first left running characteristic behind the upper head wave,

c) Interior points: those remaining in the upper characteristic net after the exclusion of (a) and (b);

d, e, f) Three similar groupings for the lower characteristic net.

In each of these cases dm_r^* is an exact differential, and therefore

$$-\int_U^1 dm_r^* = m_{r_U}^* - m_{r_1}^* \qquad (5.16)R$$

$$+\int_L^1 dm_r^* = m_{r_1}^* - m_{r_L}^*. \qquad (5.16)L$$

The difference between boundary, semi-interior and interior points enters into the several ways in which the remaining integrals of (5.15)R and (5.15)L are evaluated.

The variation in r and θ between adjacent lattice points is very small, so at the penalty of a slight decrease in accuracy it is permissible to set

$$\beta_U^{-1} = \beta_L^{-1} = \beta_1^{-1}, \quad r_U = r_L = r_1, \quad R_U = R_L = R_1, \quad S_U = S_L = S_1, \quad \cot\theta_U = \cot\theta_L = \cot\theta_1.$$

38. When point 1 in the upper characteristic net is a boundary point, the value of $m^*_{\theta_1}$ is determined by the boundary condition of tangent surface flow,

$$m^*_{\theta_1} = -\alpha M^*_S(r_1). \tag{5.17}$$

The value of $m^*_{r_1}$ is obtained by integrating along the right running characteristic, using (5.15)R, to obtain

$$m^*_{r_1} = -\beta_1^{-1}\left[1-(\theta_U-\theta_1)(R_1+\nu\cot\theta_1)\right]m^*_{\theta_1} + \left[1-R_1(\theta_U-\theta_1)\right](m^*_{r_U}+\beta_1^{-1}m^*_{\theta_U}). \tag{5.18}$$

This result simplifies when U is on the upper head wave, for then

$$m^*_{r_U} = m^*_{\theta_U} = 0, \tag{5.19}$$

and in the formula for $m^*_{r_1}$ the last term vanishes.

39. When point 1 is on the first left running characteristic downstream of the upper head wave the integration of (5.15)L along the left running characteristics offer no difficulty and is easily seen to yield

$$\left[1+R_1(\theta_1-\theta_L)\right]m^*_{r_1} - \beta_1^{-1}\left[1+\nu(\theta_1-\theta_L)\cot\theta_1\right]m^*_{\theta_1} = m^*_{r_L} - \beta_1^{-1}m^*_{\theta_L}. \tag{5.20)L}$$

The integration of (5.15)R along the right running characteristic must be considered in some detail, however, because of the condition

(5.19) which applies. In the usual two dimensional supersonic wing theory the head wave is assumed to be a line across which abrupt changes in fluid properties occur. The properties actually change gradually, across a Prandtl-Meyer fan, and the accuracy of the formulas can be improved by taking into account this more nearly correct feature of the flow.

Now, close to the leading edge the Prandtl-Meyer expansion is completed over a small fraction of the distance along the right running characteristic between U and 1, and the distance which must be traversed by the fluid to ensure complete expansion increases as the points U are taken farther from the leading edge; finally, the expansion will be so gradual that it will be complete exactly at some point, not necessarily a lattice point, on the right running characteristic through U. Although along the right running characteristics between U and 1 the m_r^* and m_θ^* change radically, from O on the head wave to non-zero values at 1, they are small in magnitude, so that some reasonable simplifying assumption about their approximate behavior may be made. To make the calculations very simple and definite it will be assumed that over the Prandtl-Meyer fan the perturbation-velocity components

1) increase in absolute value linearly from O to the proper values at the completion of the expansion, and
2) on the characteristic between U and 1 are constant between the end of the Prandtl-Meyer fan and lattice point 1.

That is, along the right running characteristic between U and 1, as the upper point occupies successively (1b), (1c), (1d),..., (see Fig. 17) the 1st, 2nd, 3rd, ... lattice points, on the upper head wave

removed from the leading edge, the variation of m_r^* and m_θ^* will appear as in Fig. 18:

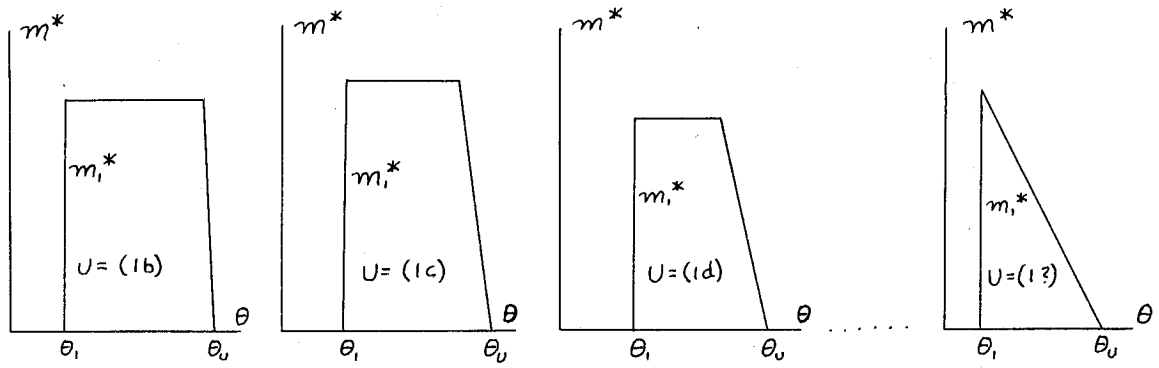

Fig. 18 - m^* is either m_r^* or m_θ^*

This assumed behavior of m_r^* and m_θ^* over the right running characteristics from U, on the head wave, to 1, on the first left running characteristic downstream of the upper head wave, is given symbolic form by writing

$$\int_U^1 m_r^*\, d\theta = -k_r\, m_{r_1}^*\, (\theta_U - \theta_1), \quad \tfrac{1}{2} \le k_r \le 1$$
$$\int_U^1 m_\theta^*\, d\theta = -k_\theta\, m_{\theta_1}^*\, (\theta_U - \theta_1), \quad \tfrac{1}{2} \le k_\theta \le 1; \tag{5.21}$$

for simplicity take

$$k_r = k_\theta = k, \qquad \tfrac{1}{2} \le k \le 1 \tag{5.22}$$

Thus, when the point 1 at which m_r^* and m_θ^* are to be computed is on the first left running characteristic downstream of the upper head wave the compatibility equation (5.15)R is particularized to

$$-m_{r_1}^* - \beta_1^{-1} m_{\theta_1}^* - R_1\, k\, m_{r_1}^*\, (\theta_U - \theta_1) + \nu k \beta_1^{-1} \cot\theta_1\, m_{\theta_1}^*\, (\theta_U - \theta_1) = 0. \tag{5.23R}$$

Combining terms yields

$$\left[1 + k R_1\, (\theta_U - \theta_1)\right] m_{r_1}^* + \beta_1^{-1} \left[1 - \nu k \cot\theta_1\, (\theta_U - \theta_1)\right] m_{\theta_1}^* = 0,$$

and solving for $m_{r_1}^*$ results in

$$m_{r_1}^* = -\beta_1^{-1}\left[1-K(\theta_U-\theta_1)(R_1+\nu\cot\theta_1)\right]m_{\theta_1}^*, \qquad (5.24)R$$

after neglecting terms in which $\theta_U-\theta_1$, which is $<<1$, enters with an exponent greater than one.

It is most convenient to employ a constant Mesh angle, and in that event $\theta_U-\theta_1$ and $\theta_1-\theta_L$ will be equal except when L is on the upper surface of the wing and is not a lattice point. For that (single) case it is not worth while to solve equations (5.20)L and (5.24)R simultaneously for $m_{r_1}^*$ and $m_{\theta_1}^*$. However, for all other situations U, L and 1 will be lattice points and

$$\theta_U-\theta_1=\theta_1-\theta_L=\Delta\theta\ ;$$

then the values of $m_{r_1}^*$ and $m_{\theta_1}^*$ are given as

$$m_{r_1}^* = \tfrac{1}{2}\left[1-(1+K)\tfrac{\Delta\theta}{2}(R_1+\nu\cot\theta_1)\right](m_{r_L}^*-\beta_1^{-1}m_{\theta_L}^*) \qquad (5.25)r$$

$$m_{\theta_1}^* = \tfrac{1}{2}\beta_1\left[1-(1-K)\tfrac{\Delta\theta}{2}(R_1+\nu\cot\theta_1)\right](m_{r_L}^*-\beta_1^{-1}m_{\theta_L}^*). \qquad (5.25)\theta$$

40. When 1 is an interior point of the upper characteristic net the several integrals in (5.15)L and (5.15)R are approximately evaluated by the Mean Value Theorem for Integrals to give

$$\left[1+R_1(\theta_U-\theta_1)\right]m_{r_1}^*+\beta_1^{-1}\left[1-\nu(\theta_U-\theta_1)\cot\theta_1\right]m_{\theta_1}^* = m_{r_U}^*+\beta_1^{-1}m_{\theta_U}^* \qquad (5.26)R$$

$$\left[1+R_1(\theta_U-\theta_L)\right]m_{r_1}^*-\beta_1^{-1}\left[1+\nu(\theta_1-\theta_L)\cot\theta_1\right]m_{\theta_1}^* = m_{r_L}^*-\beta_1^{-1}m_{\theta_L}^* \qquad (5.26)L$$

In the upper characteristic net there will be one pair of points U and L for which L is on the upper airfoil surface. For that case, if L is not a lattice point, the general equations (5.26)R and (5.26)L are

solved for $m^*_{r_1}$ and $m^*_{\theta_1}$.

However, when L is a lattice point, and for all other points in the interior of the upper characteristic net,

$$\theta_U - \theta_1 = \theta_1 - \theta_L = \Delta\theta,$$

as before, and the compatibility equations are readily solved to yield

$$m^*_{r_1} = \frac{m^*_{r_U} + m^*_{r_L}}{2}(1 - R_1\Delta\theta) + \frac{\beta_1^{-1}}{2}(m^*_{\theta_U} - m^*_{\theta_L}) \qquad (5.27)\,r$$

$$m^*_{\theta_1} = \frac{m^*_{\theta_U} + m^*_{\theta_L}}{2} + \frac{\beta_1}{2}(m^*_{r_U} - m^*_{r_L}), \qquad (5.27)\,\theta$$

after neglecting second order and higher terms in $\Delta\theta$ and discarding

$$-\frac{\beta_1^{-1}}{2} R_1 \Delta\theta\,(m^*_{\theta_U} - m^*_{\theta_L}),$$

which will be negligible compared to the other terms in (5.27)r.

41. With the same approximations as those employed in the derivation of the compatibility equations for the upper characteristic net it is easy to establish the following results for the lower characteristic net.

a) When 1 is a boundary point

$$m^*_{\theta_1} = -\alpha\, M^*_S(r_1)$$
$$m^*_{r_1} = \beta_1^{-1}\left[1-(\theta_1-\theta_L)(R_1 - \nu\cot\theta_1)\right] m^*_{\theta_1} + \left[1 - R_1(\theta_1-\theta_L)\right](m^*_{r_L} - \beta_1^{-1} m^*_{\theta_L}).$$

The formula for $m^*_{r_1}$ simplifies when L is on the lower head wave, for then

$$m^*_{r_L} = m^*_{\theta_L} = 0$$

b) When is on the first right running characteristic downstream of the lower head wave

$$m^*_{r_1} + \beta_1^{-1}\left[1-(R_1+\nu\cot\theta_1)(\theta_U-\theta_1)\right] m^*_{\theta_1} = \left[1 - R_1(\theta_U-\theta_1)\right](m^*_{r_U} + \beta_1^{-1} m^*_{\theta_U}$$
$$m^*_{r_1} - \beta_1^{-1}\left[1 - K(R_1 - \nu\cot\theta_1)(\theta_1-\theta_L)\right] m^*_{\theta_1} = 0, \qquad (\tfrac{1}{2} \le K \le 1).$$

These equations are readily solved when U, L, 1 are lattice points, for which

$$\theta_U - \theta_1 = \theta_1 - \theta_L = \Delta\theta ;$$

then,

$$m^*_{r_1} = \tfrac{1}{2}\left[1 + (1-k)\tfrac{\Delta\theta}{2}(R_1 - \nu \cot\theta_1)\right](m^*_{r_U} + \beta_1^{-1} m^*_{\theta_U})$$
$$m^*_{\theta_1} = \tfrac{\beta_1}{2}\left[1 + (1+k)\tfrac{\Delta\theta}{2}(R_1 - \nu \cot\theta_1)\right](m^*_{r_U} + \beta_1^{-1} m^*_{\theta_U}).$$

c) When 1 is an interior point of the lower characteristic net the compatibility equations (5.26)R and (5.26)L are solved for $m^*_{r_1}$ and $m^*_{\theta_1}$. For the case where U, L, 1 are lattice points the compatibility equations are readily solved to yield (5.27)r and (5.27)θ, the same as for the upper net.

42. As numerical examples of the Method of Characteristics the linearized supersonic source flow over each of a ring- and annular-wing will be computed. So that the results for the annular wing can be compared with those obtained by the use of the Riemann method, the numerical data of section 30 will be assumed.

The ring wing is chosen to have zero thickness and to have the form of the lateral surface of a right circular cylinder, its axis collinear with the symmetry axis of the rocket motor. Then at a given point on the wing the angle of attack is actually the angle θ between the axis of symmetry and the streamline to the point. The streamline that intersects the leading edge makes an angle of 6° with the ring axis.

In section 30 the annular wing is described.

43. The characteristics of the disturbed flow, which were shown to be the characteristics of the source flow, are readily constructed by the use of Fig. 11, using a mesh angle of 15' for part of the wing and a mesh angle of 30' for the rest. This is considered to be sufficiently fine to obviate the necessity of iterating to improve the results. Actually, only the lattice points on the head waves need be claculated, all other lattice points being determined by construction, since $M_s(r)$ and hence the Mach angle μ are constant over spherical surfaces with centers at the source.

In Figs. 19 and 21 the network of characteristics surrounding the trace of the ring wing of the numerical example are exhibited, and Figs. 20 and 22 show the characteristic net constructed about the annular wing of the numerical example. From the figures it is clear that in the two examples the orientations of the surfaces to the supersonic source flow are identical.

The chord of the ring wing is not so great, however, that the head wave interior to the ring will reflect off of the symmetry axis and intersect the wing (see Fig. 21), so interference with the interior surface is avoided.

Although with the annular wing the possibility of interference due to waves reflected from the axis of symmetry does not exist, there is the chance that waves reflected from the nozzle walls can strike the airfoil. Of course, this type of interference can also occur when the ring wing is in the main stream. To eliminate the possibility that waves reflected from the walls will intersect either the ring- or annular- wing of the examples the upper characteristic nets in both cases

have as their highest lattice points the intersection of the upper head wave with the radial streamline which is at an angle of 9° to the nozzle axis. This is equivalent to assuming that each type of airfoil is set in a nozzle with an expansion half-angle of 9°, which is about the optimum. When the ring- and annular- wings of the numerical examples have 10-unit chords, the leading edge head wave reflected from the nozzle walls will just graze the trailing edges.

44. For the upper characteristic net when U is on the upper head wave, and for the lower characteristic net when L is on the lower head wave, the values of K as a function of position on the head wave will be assumed as below.

Point on Head Wave		Value of K
Upper	Lower	
1b	2a	1.0
1c	3a	0.9
1d	4a	0.8
1e	5a	0.7
1f	6a	0.6
1g	7a	0.5
1h	8a	0.7
1i	9a	0.6
1j	10a	0.5

The results of the computations are not too sensitive to the value assigned to K, for K always enters the compatibility equations as a coefficient of $\theta_U - \theta_1$, or $\theta_1 - \theta_L$, which are of the order of 0.004, which is then added to or subtracted from unity.

45. For the purposes of computing the perturbed supersonic source flow about the ring- and annular- wings of the numerical examples the curves

in Figs. 23 - 26 are useful.

As has been noted previously, the difference in the ring- and annular- airfoils shows up in the comparative values of $\cot\theta$, which are large for the ring wing and negligibly small for the annular wing. The same compatibility equations are used for the two cases, except that when the ring wing is considered, $\nu = 1$, which requires the computation of $\cot\theta$; when the annular wing is in the source flow, $\nu = 0$, which allows the $\cot\theta$ term to be neglected.

46. Figures 27 - 31 contain the end results of the numerical work. The first Figure (27) exhibits $m^*_{\theta_1}$ on both surfaces of either the ring- or annular- airfoils of the numerical example, computed from the boundary condition

$$m^*_{\theta_1} = -\alpha\, M^*_s(r_1)$$

where α is the angle of attack (6°) at the leading edge. In Fig. 28 the values of $m^*_{r_1}$ on the upper and lower surfaces of the ring- and annular- wings are shown, together with a comparison of the analogous quantity,

$$\Delta M^*_s(r) = \pm \frac{\alpha\, M^*_s(r)}{\sqrt{M^{*2}_s(r) - 1}} ,$$

from the theory of linearized locally rectilinear flow. The third Figure (30) presents the critical Mach number M^* of the disturbed flow on the upper and lower surfaces of the ring- and annular- wings as a function of the distance from the source, as computed from formula (3.8) with the use of Fig. 29. In the same Figure there is shown, for comparison, the value of M^* given from (3.13) for linearized locally

rectilinear flow. Figure 31 offers the pressure coefficients, based on the local dynamic pressure in the source flow, of the ring- and annular-wings of the numerical examples for comparison with that of the same wing in a linearized locally rectilinear flow. In the last Figure, 31, the pressure coefficient based on the stagnation pressure is shown for the same three cases of the three preceding Figures.

APPENDIX

ATTEMPT AT A SOLUTION OF EQUATION (3.6) BY THE METHOD OF SEPARATION OF VARIABLES

In the solution of equation (3.6) the method of separation of variables is not a useful technique because of the difficulty of applying the boundary conditions, especially on the surface of the wing. The procedure is briefly discussed in this Appendix in order that the difficulties may be exhibited.

The method of separation of variables is employed to solve equation (3.6) when a solution is sought in the form of a product of a function R of W alone and a function T of θ alone; that is, when it is assumed that

$$\mathcal{E}(W,\theta) \equiv R(W)\,T(\theta), \tag{A.1}$$

with $R(W)$ and $T(\theta)$ to be determined. When the assumed solution (A.1) is set into (3.6) the left and right hand members are by definition identical and there results, after dividing by $R(W)T(\theta)$,

$$\frac{8\lambda^2 W^2(1-W)}{W-\lambda^2}\,\frac{R''(W)}{R(W)} + \frac{2W[2\lambda^2(1-W)-(W-\lambda^2)]}{W-\lambda^2}\,\frac{R'(W)}{R(W)} \equiv \frac{1}{2T(\theta)\sin\theta}\,\frac{d}{d\theta}\left(T'(\theta)\sin\theta\right) \tag{A.2}$$

The common value of the two members of (A.2) is a constant, say $-\frac{n(n+1)}{2}$; hence in place of the single linear partial differential equation (3.6) two linear ordinary differential equations are obtained:

$$\frac{d}{d\theta}\left(T'(\theta)\sin\theta\right) + n(n+1)\sin\theta\;T(\theta) = 0, \tag{A.3}$$

$$W^2(1-W)R''(W) + W\left[\frac{3}{4} - \frac{1+2\lambda^2}{4\lambda^2}W\right]R'(W) + \frac{n(n+1)}{16\lambda^2}(W-\lambda^2)R(W) = 0. \tag{A.4}$$

Equation (A.3) is the wellknown Legendre differential equation, with the linearly independent solutions (n is a positive integer or zero)

$$P_n(\cos\theta), \quad Q_n(\cos\theta),$$

the Legendre functions of the first and second kinds, respectively, of index n. Hence the solution of (A.3) is

$$T(\theta) = c_1 P_n(\cos\theta) + c_2 Q_n(\cos\theta). \tag{A.5}$$

Equation (A.4) is of the form

$$w^2(w-1)R''(w) + w\left[(\alpha+\beta-1) + (a+b+1)w\right]R'(w) + ab\left(w - \frac{\alpha\beta}{ab}\right)R(w) = 0, \tag{A.4}'$$

with regular singular points at 0, 1, ∞, and so it can be anticipated that the solution of equation (A.4)' is related to the hypergeometric function.

To obtain one solution of equation (A.4)' first make the substitution

$$R(w) = w^{\alpha} S_1(w);$$

the differential equation satisfied by $S_1(w)$ is then

$$w(1-w)S_1''(w) + \left[(\alpha-\beta+1) - (a+\alpha+b+\alpha+1)w\right]S_1'(w) - (a+\alpha)(b+\alpha)S_1(w) = 0,$$

the hypergeometric equation of Gauss, with one solution given by

$$S_1(w) = F(a+\alpha, b+\alpha; \alpha-\beta+1; w),$$

and so a solution of (A.4)' is the function

$$R_1(w) = w^{\alpha} F(a+\alpha, b+\alpha; \alpha-\beta+1; w).$$

A second solution of equation (A.4)' is obtained by use of the substitution

$$R(w) = w^{\beta} S_2(w)$$

the differential equation satisfied by $S_2(w)$ is

$$w(1-w)S_2''(w) + \left[(\beta-\alpha+1) - (a+\beta+b+\beta+1)w\right]S_2'(w) - (a+\beta)(b+\beta)S_2(w) = 0,$$

which is also the hypergeometric equation, one solution of which is

$$S_2(w) = F(a+\beta,\ b+\beta;\ \beta-\alpha+1;\ w),$$

and hence the second solution of (A.4)' is the function

$$R_2(w) = w^{\beta} F(a+\beta,\ b+\beta;\ \beta-\alpha+1;\ w).$$

When $\alpha \neq \beta$ and $\alpha-\beta$ is not a positive integer (which is the case here) the general solution of equation (A,4)' is

$$R(w) = c_3 w^{\alpha} F(a+\alpha, b+\alpha; \alpha-\beta+1; w) + c_4 w^{\beta} F(a+\beta, b+\beta; \beta-\alpha+1; w). \qquad (A.6)$$

From (A.6), by comparing the coefficients of equations (A.4) and (A.4)', the solution of the former differential equation is given by

$$R(w) = c_3 w^{-\frac{n}{4}} F\left(a-\tfrac{n}{4}, b-\tfrac{n}{4}; \tfrac{-2n+3}{4}; w\right) + c_4 w^{\frac{n+1}{4}} F\left(a+\tfrac{n+1}{4}, b+\tfrac{n+1}{4}; \tfrac{2n+5}{4}; w\right), \qquad (A.7)$$

where

$$a+b = \frac{1-2\lambda^2}{4\lambda^2}$$
$$ab = -\frac{n(n+1)}{16\lambda^2} \qquad (A.8)$$

Since the general solutions of the ordinary differential equations in the separated angular and radial variables are known in (A.5) and (A.7) respectively, the general solution of equation (3.6) is given by

$$\mathcal{E}(w,\theta) = \sum_{n=0}^{\infty} \left[c_1 P_n(\cos\theta) + c_2 Q_n(\cos\theta)\right]\left[c_3 w^{-\frac{n}{4}} F\left(a-\tfrac{n}{4}, b-\tfrac{n}{4}; \tfrac{-2n+3}{4}; w\right) + c_4 w^{\frac{n+1}{4}} F\left(a+\tfrac{n+1}{4}, b+\tfrac{n+1}{4}; \tfrac{2n+5}{4}; w\right)\right] \qquad (A.9)$$

with a and b defined through (A.8).

In order to apply the boundary condition over the surface of the wing it is necessary to establish an orthogonality relation which can be used to evaluate some of the arbitrary constants of (A.9). For either the ring or annular wing this boundary condition is employed in the usual manner, not on the wing itself but on some simple approximating surface, in this instance on a surface with constant angle θ_o for the

range of values assumed by w between the leading and trailing edges. In the case of the ring wing this constant angle θ_o gives the conical surface, with vertex at the source, to which the ring is presumed to approximate; for the annular wing $\theta_o = \frac{\pi}{2}$, so that the boundary condition is applied on the x, y plane.

As will appear, an orthogonality condition cannot be constructed in the usual manner and hence it is not possible to apply the required boundary condition,

$$\mathcal{E}_\theta(w, \theta_o) = r\alpha\, \phi'(r),$$

where α is the angle of attack of the wing.

Thus, from (A.9), the boundary condition above requires that

$$\mathcal{E}_\theta(w, \theta_o) = -\sin\theta_o \sum_{n=0}^{\infty}{}' \Big[g_n w^{-\frac{n}{4}} F\left(a-\tfrac{n}{4},\, b-\tfrac{n}{4};\, \tfrac{-2n+3}{4};\, w\right) + h_n w^{\frac{n+1}{4}} F\left(a+\tfrac{n+1}{4},\, b+\tfrac{n+1}{4};\, \tfrac{2n+5}{4};\, w\right)\Big] = r\alpha\,\phi'(r).$$

In the attempt to construct an orthogonality relation satisfied by the solutions of equation (A.4), after calculation of the appropriate integrating factor that differential equation takes the self-adjoint form

$$\frac{d}{dw}\left[w^{\frac{3}{4}}(1-w)^{\frac{1-\lambda^2}{4\lambda^2}} R'(w)\right] + \frac{n(n+1)}{16\lambda^2}\,\frac{(w-\lambda^2)(1-w)^{\frac{1-5\lambda^2}{4\lambda^2}}}{w^{\frac{5}{4}}}\, R(w) = 0 \qquad \text{(A.10)}$$

Equation (A.10) is written in the two forms

$$\frac{d}{dw}\left[w^{\frac{3}{4}}(1-w)^{\frac{1-\lambda^2}{4\lambda^2}} R_m'(w)\right] + \frac{m(m+1)}{16\lambda^2}\,\frac{(w-\lambda^2)(1-w)^{\frac{1-5\lambda^2}{4\lambda^2}}}{w^{\frac{5}{4}}}\, R_m(w) = 0 \qquad \text{(A.10}_1\text{)}$$

$$\frac{d}{dw}\left[w^{\frac{3}{4}}(1-w)^{\frac{1-\lambda^2}{4\lambda^2}} R_n'(w)\right] + \frac{n(n+1)}{16\lambda^2}\,\frac{(w-\lambda^2)(1-w)^{\frac{1-5\lambda^2}{4\lambda^2}}}{w^{\frac{5}{4}}}\, R_n(w) = 0. \qquad \text{(A.10}_2\text{)}$$

Multiply (A.10$_1$) by $R_n(w)$ and multiply (A.10$_2$) by $R_m(w)$ and subtract, then integrate throughout the entire supersonic region, from $w = \lambda^2$ to $w = 1$ to get

$$\int_{\lambda^2}^{1} \left[R_n(w) \frac{d}{dw} \left\{ w^{\frac{3}{4}}(1-w)^{\frac{1-\lambda^2}{4\lambda^2}} R'_m(w) \right\} - R_m(w) \frac{d}{dw} \left\{ w^{\frac{3}{4}}(1-w)^{\frac{1-\lambda^2}{4\lambda^2}} R'_n(w) \right\} \right] dw$$

$$+ \frac{m(m+1)-n(n+1)}{16\lambda^2} \int_{\lambda^2}^{1} \frac{(w-\lambda^2)(1-w)^{\frac{1-5\lambda^2}{4\lambda^2}}}{w^{\frac{5}{4}}} R_m(w) R_n(w)\, dw = 0 \qquad \text{(A.11)}$$

Integrating the first integral by parts reduces (A.11) to

$$\frac{m(m+1)-n(n+1)}{16\lambda^2} \int_{\lambda^2}^{1} \frac{(w-\lambda^2)(1-w)^{\frac{1-5\lambda^2}{4\lambda^2}}}{w^{5/4}} R_m R_n\, dw = \lambda^{\frac{5}{2}}(1-\lambda^2)^{\frac{1-\lambda^2}{4\lambda^2}} \left[R_m(\lambda^2) R'_n(\lambda^2) - R'_m(\lambda^2) R_n(\lambda^2) \right]. \qquad \text{(A.12)}$$

Now $R_m(w)$ and $R_n(w)$ are any solutions of the differential equation (A.10), or its equivalent, (A.4). Choosing

$$R_m(w) = w^{-\frac{m}{4}} F\left(a - \tfrac{m}{4},\ b - \tfrac{m}{4};\ \tfrac{-2m+3}{4};\ w\right)$$

$$R_n(w) = w^{-\frac{n}{4}} F\left(a - \tfrac{n}{4},\ b - \tfrac{n}{4};\ \tfrac{-2n+3}{4};\ w\right),$$

the tern in brackets on the right hand side of (A.12) becomes

$$R_m(\lambda^2) R'_n(\lambda^2) - R'_m(\lambda^2) R_n(\lambda^2) = \lambda^{\frac{-n+m}{2}} \left(\frac{\lambda^2-1}{4\lambda^2}\right) \left[\frac{n(n+2)}{3-2n} F\left(a - \tfrac{m}{4},\ b - \tfrac{m}{4};\ \tfrac{-2m+3}{4};\ \lambda^2\right) \cdot \right.$$

$$\left. \cdot F\left(a - \tfrac{n-4}{4},\ b - \tfrac{n-4}{4};\ \tfrac{-2n+7}{4};\ \lambda^2\right) - \frac{m(m+2)}{3-2m} F\left(a - \tfrac{n}{4}, b - \tfrac{n}{4}; \tfrac{-2n+3}{4}; \lambda^2\right) F\left(a - \tfrac{m-4}{4}, b - \tfrac{m-4}{4}; \tfrac{-2m+7}{4}; \lambda^2\right) \right]$$

$$- \lambda^{\frac{-4+(m+n)}{2}} F\left(a - \tfrac{m}{4}, b - \tfrac{m}{4}; \tfrac{-2m+3}{4}; \lambda^2\right) F\left(a - \tfrac{n}{4}, b - \tfrac{n}{4}; \tfrac{-2n+3}{4}; \lambda^2\right) \left[\tfrac{n-m}{4} \right].$$

Clearly then, the right hand member of (A.12) does not vanish, so that the functions $R_m(w)$ and $R_n(w)$ are not orthogonal in the range $\lambda^2 \le w \le 1$ and thus there is no simple way of applying the boundary condition which requires that the flow over the wing be tangent to the wing surface.

An added complication is the difficulty of applying the condition that only outgoing waves leave the upper and lower surfaces of the airfoil. There seems to be no direct method of choosing the undetermined constants in (A.9) so that the solution has this required property.

REFERENCES

1. Tsien, H. S.: Symmetrical Joukowsky Airfoils in Shear Flow. Quarterly of Applied Mathematics, Vol. I, pp. 130-148, 1943.

2. von Karman, Th. and Tsien, H. S.: Lifting-Line Theory for a Wing in Non-Uniform Flow. Quarterly of Applied Mathematics, Vol. III, pp. 1-11, 1945.

3. Mirels, Harold: Theoretical Method for Solution of Aerodynamic Forces on Thin Wings in Non-Uniform Supersonic Stream with an Application to Tail Surfaces. NACA TN 1736, November 1948.

4. Ferrari, C.: Determination of the Pressure on a Solid of Revolution with a Pointed Nose in Supersonic Yawing Motion. Atti della R. Academia delle Scienze di Torino, Vol 72, pp. 140-163, 1936-37.

5. Tsien, H. S.: Supersonic Flow over an Inclined Body of Revolution. Jour. Aero. Sciences, pp. 480-483, 1938.

6. Sauer, R.: Uberschallstromung um beliebeg geformte Geschossspitzen unter kleinem Anstellwinkel. Luftfahrtforschung, Vol. 19, pp. 148-152, May 1942.

7. Stone, A. H.: On Supersonic Flow Past a Slightly Yawing Cone. Jour. of Math. and Phys., Vol. XXVII, pp. 67-81, 1948.

8. Liepmann, H. W. and Puckett, A. E.: Aerodynamics of a Compressible Fluid. John Wiley and Sons, New York, 1947.

9. Lagrange, J. P.: Memoire sur la Theorie du Movement des Fluides. Nouv. Mem. de l'Acad. de Berlin, 1781.

10. Courant, R. and Friedrichs, K.: Supersonic Flow and Shock Waves. Interscience Publishers, Inc., New York, 1948.

11. Van Dyke, M. D.: A Study of Second Order Supersonic Flow. Ph.D. Thesis, California Institute of Technology, Pasadena, California, 1949.

12. Bateman, H.: Partial Differential Equations of Mathematical Physics. Dover Press, New York, 1943.

13. Courant, R. and Hilbert, D.: Methoden der Mathematichen Physik. Vol. II, Interscience Publishers, Inc., New York, 1943.

14. Frank, P. and von Mises, R.: Die Differential-und Integralgleichungen der Mechanik und Physik. Vol. I, Friedr. Vieweg & Sohn, Braunschweig, 1930.

15. Hadamard, J.: Lectures on Cauchy's Problem in Linear Partial Differential Equations. Yale University Press, New Haven, Connecticut, 1923.

16. Riemann, B.: Uber die Fortpflanzung ebener Luftwellen von endicher Schwingungsweite. Gottingen Abhandl, 8, 1860; also Werke, p. 145.

17. Webster, A. G.: Partial Differential Equations of Mathematical Physics. G. E. Stechert and Co., New York, 1933.

18. Hayes, W. D.: Linearized Supersonic Flow. Ph.D. Thesis, California Institute of Technology, Pasadena, California, 1947.

19. Temple, G. and Jahn, H. A.: Flutter at Supersonic Speeds: Derivative Coefficients for a Thin Airfoil at Zero Incidence. R. & M. No. 2140, 1949.

20. Gray, A., Mathews, G. B. and Macrobert, T. M.: Bessel Functions. Macmillan and Co., Ltd., London, 1931.

21. Prandtl, L. and Busemann, A.: Näherungsverfahren zur Zeichnerischen Ermittlung von ebenen Strömungen mit Uberschallgeschwindigkeit. Stoloda Festschrift, Zurich, 1929.

22. Busemann, A.: Gasdynamik. Handbuch der Experimental Physik, Band IV, 1, Leipzig, 1931.

23. Frankl, F. I.: Supersonic Flows with Axial Symmetry. Izvetia Akademii RKKA (Russian), Vol. I, 1934.

24. Ferrari, C.: Campo Aerodinamico a velocita iperacustica attorno a un solido di rivoluzione a prora acuminata. L'Aerotecnica, Vol. XVI, fasc, 2, Feb. 1936.

25. Guderly, G.: Die Characteristikenmethode fur ebenen und achsensymmetrische Uberschallströmungen. Jahrbuch 1940 der deutsche Luftfahrtforschung, R. Oldenbourg, Munich.

26. Sauer, R.: Charakteristikenverfahren fur raumliche achsensymmetrische Uberschallströmungen. Forschungsbericht M. 1269, Göttingen, 1940. (Translated as NACA TM 1133, January, 1947.).

27. Miller, F. H.: Partial Differential Equations. John Wiley & Sons, New York, 1941.

Rasof_b_1950

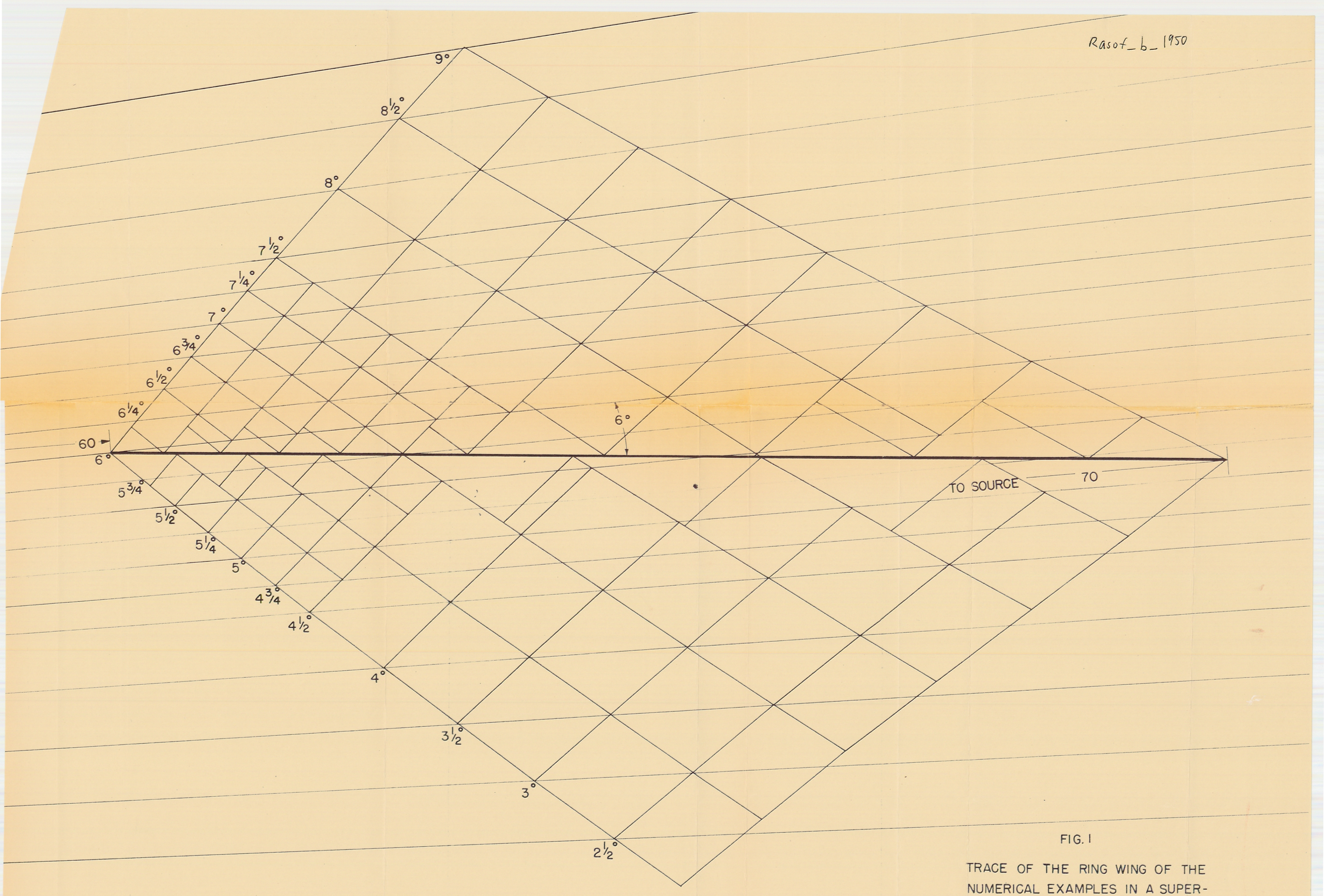

FIG. 1

TRACE OF THE RING WING OF THE NUMERICAL EXAMPLES IN A SUPERSONIC SOURCE FLOW, SHOWING THE CHARACTERISTIC NETS IN THE COMPUTATIONS

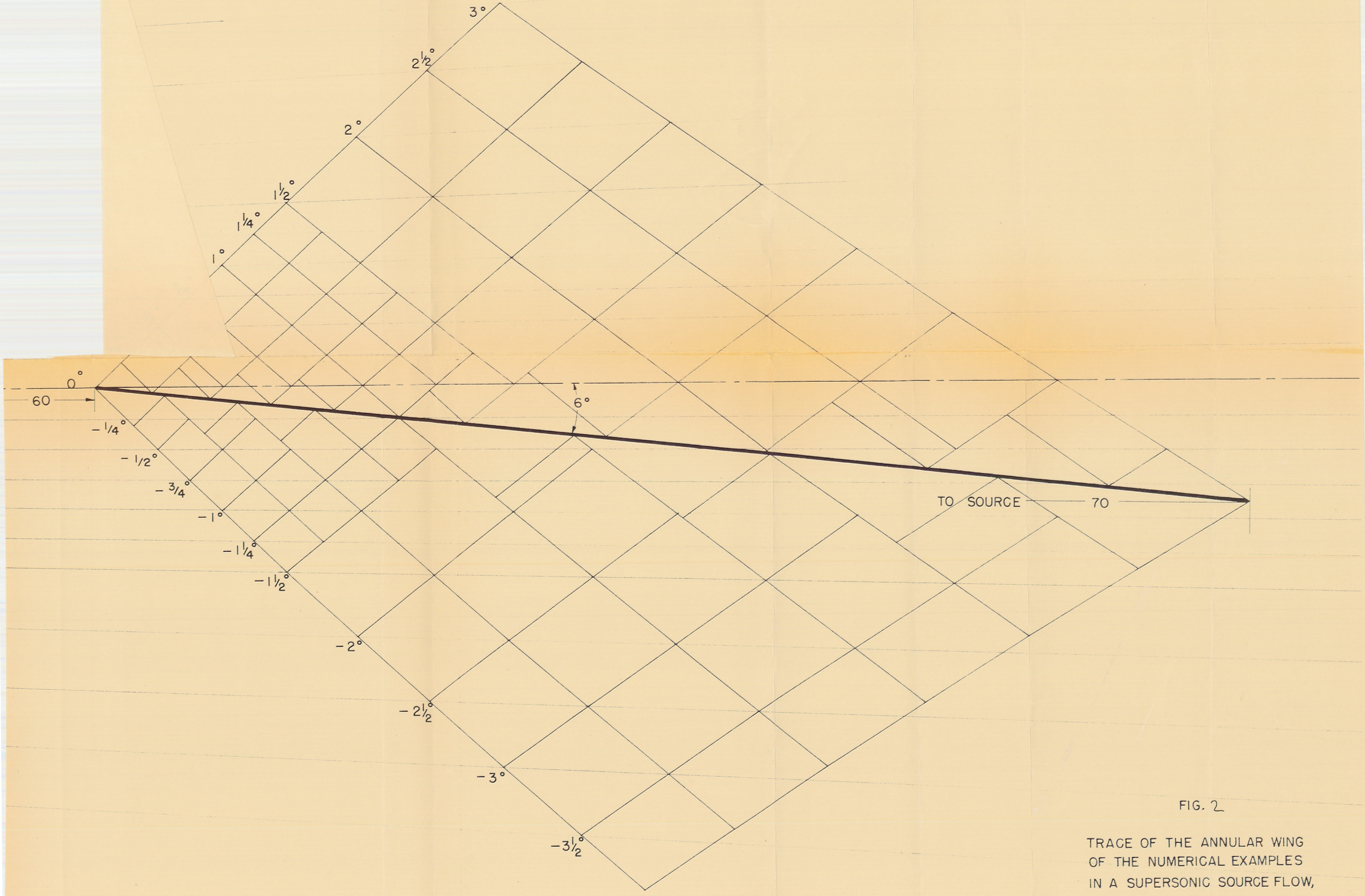

FIG. 2

TRACE OF THE ANNULAR WING OF THE NUMERICAL EXAMPLES IN A SUPERSONIC SOURCE FLOW, SHOWING THE CHARACTERISTIC NETS USED IN THE COMPUTATIONS

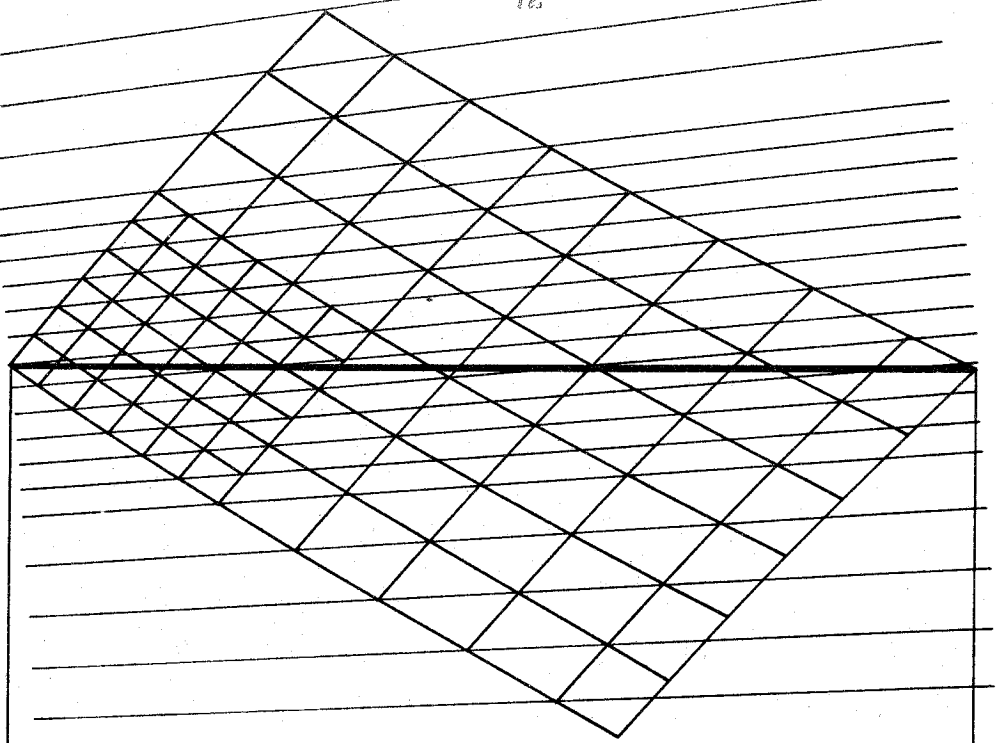

Fig. 21 - Sketch of the Characteristic Nets and Traces of the Ring Wing of the Numerical Examples

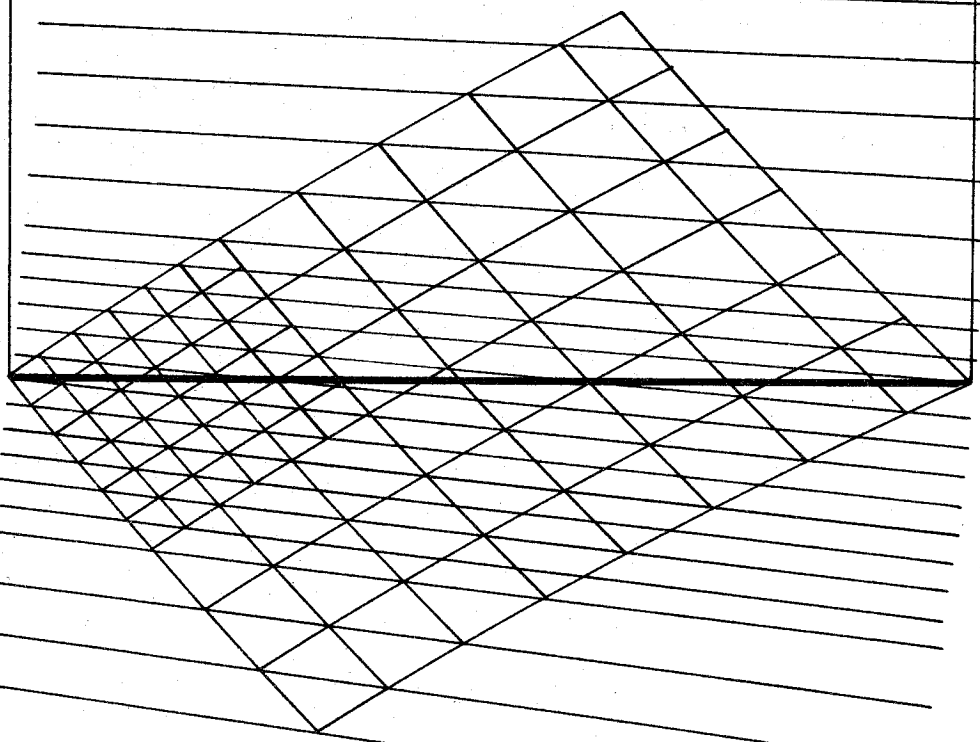

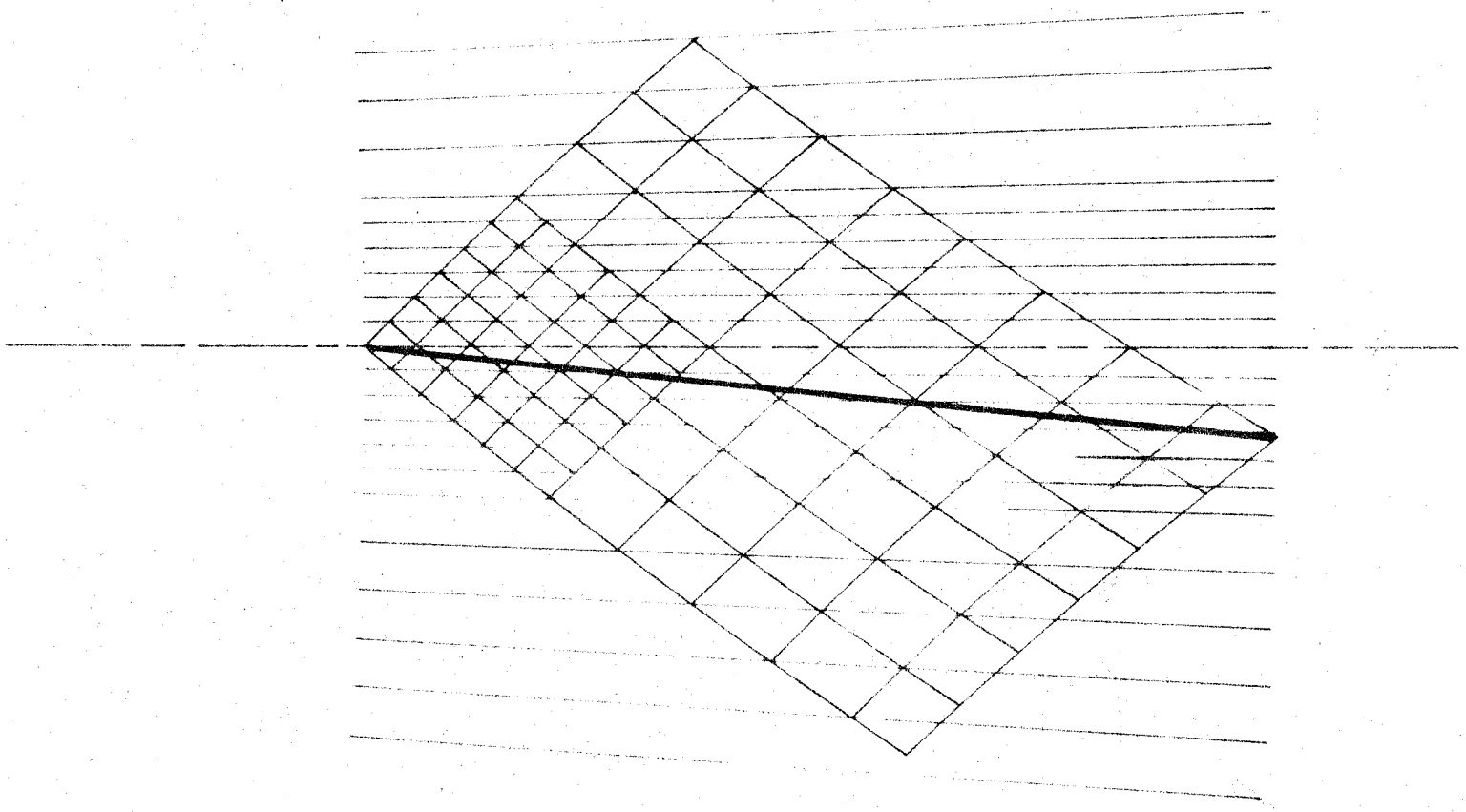

Fig. 22 - Sketch of the Characteristic Net and Trace of the Annular Wing of the Numerical Examples

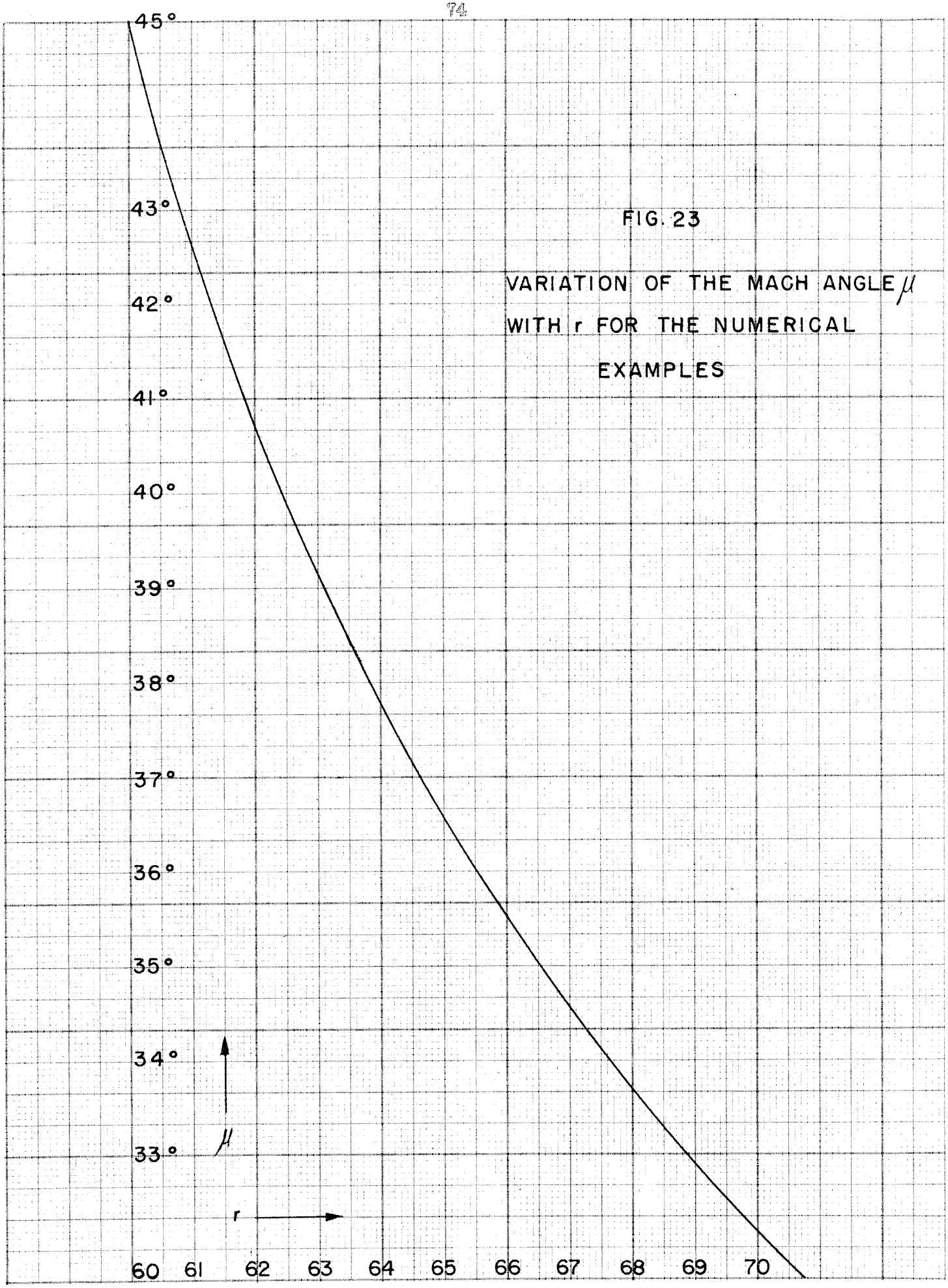

FIG. 23

VARIATION OF THE MACH ANGLE μ WITH r FOR THE NUMERICAL EXAMPLES

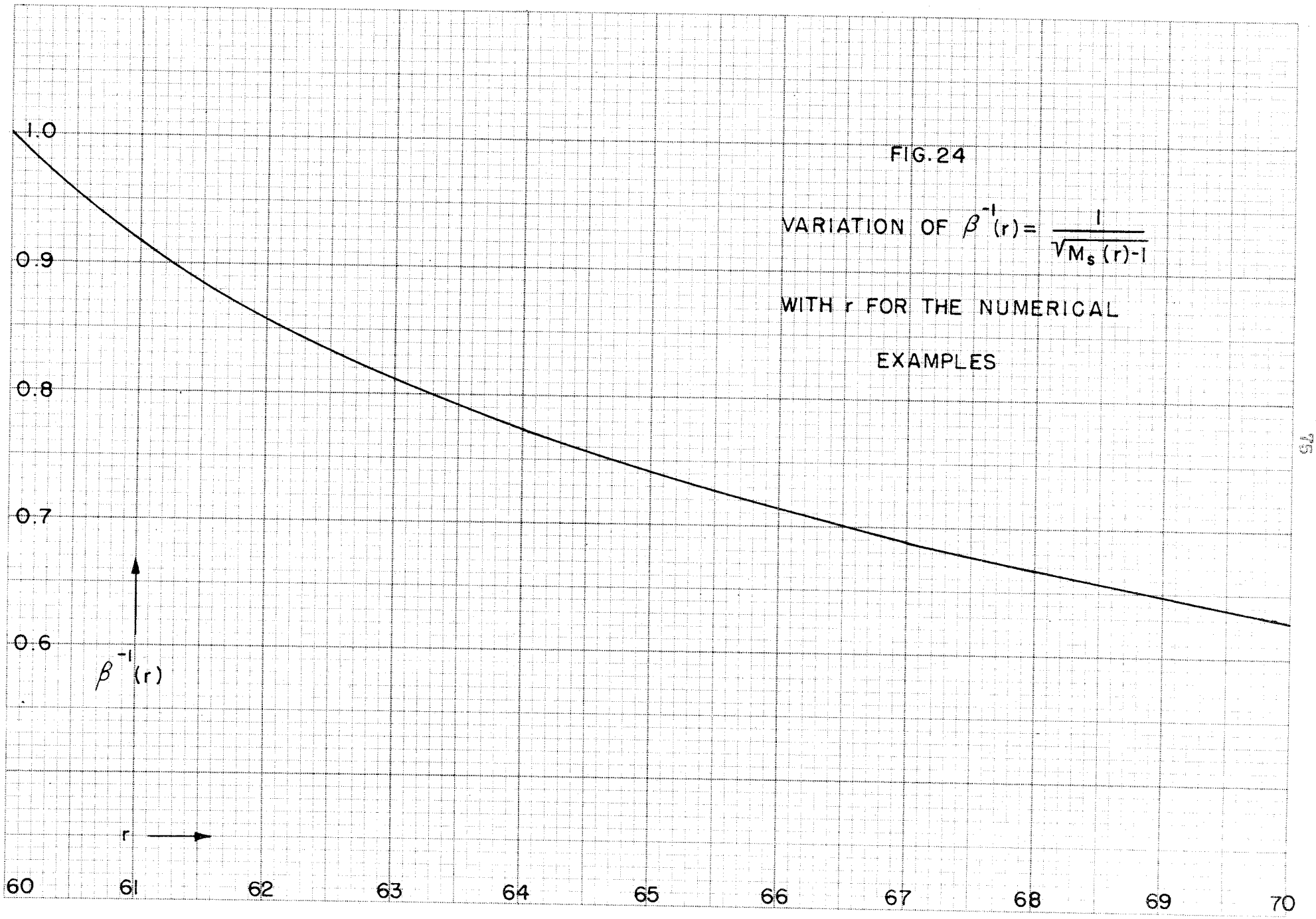

FIG. 24

VARIATION OF $\beta^{-1}(r) = \frac{1}{\sqrt{M_s(r)-1}}$

WITH r FOR THE NUMERICAL

EXAMPLES

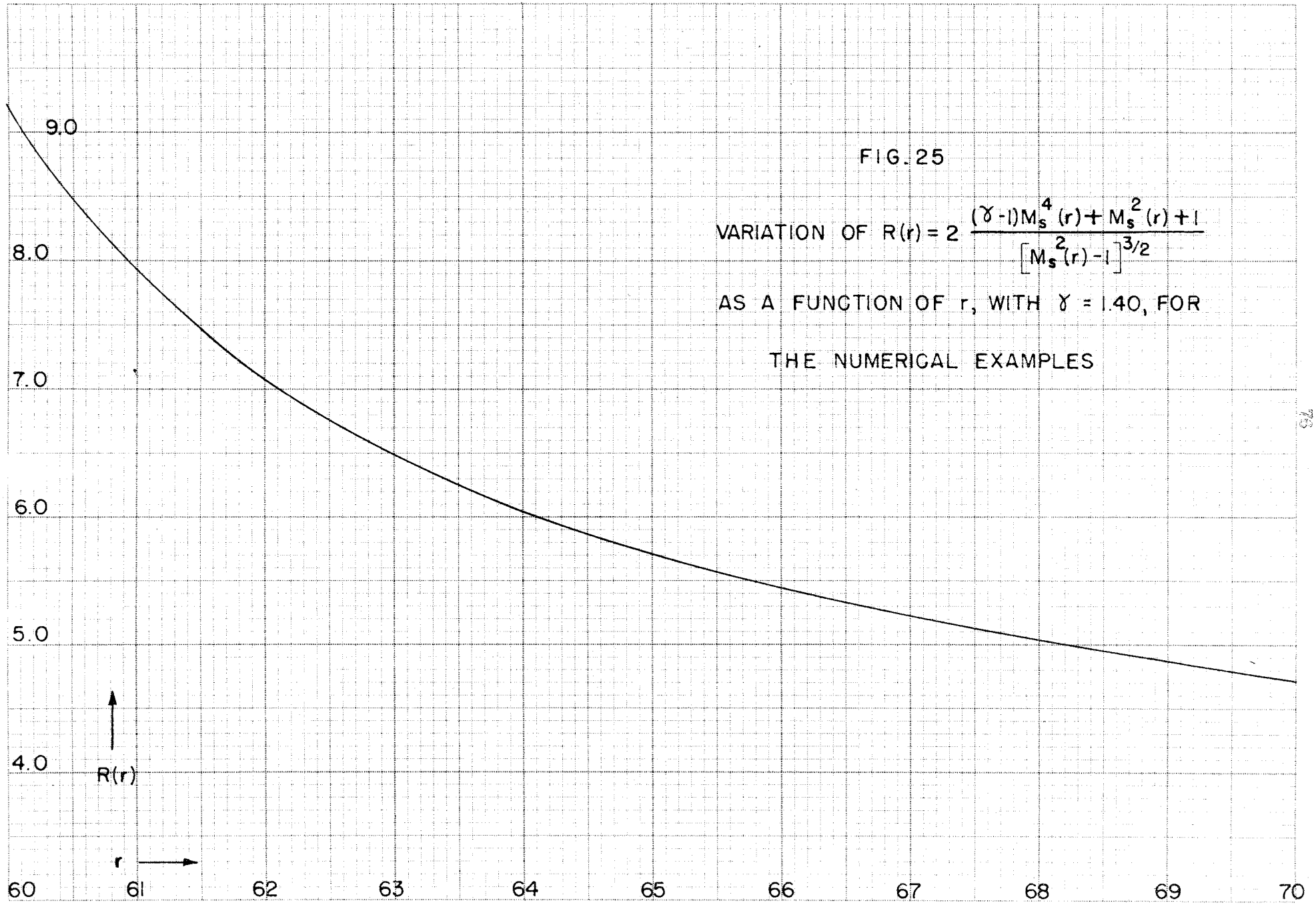

FIG. 25

VARIATION OF $R(r) = 2\,\dfrac{(\gamma-1)M_s^4(r) + M_s^2(r) + 1}{\left[M_s^2(r)-1\right]^{3/2}}$

AS A FUNCTION OF r, WITH $\gamma = 1.40$, FOR

THE NUMERICAL EXAMPLES

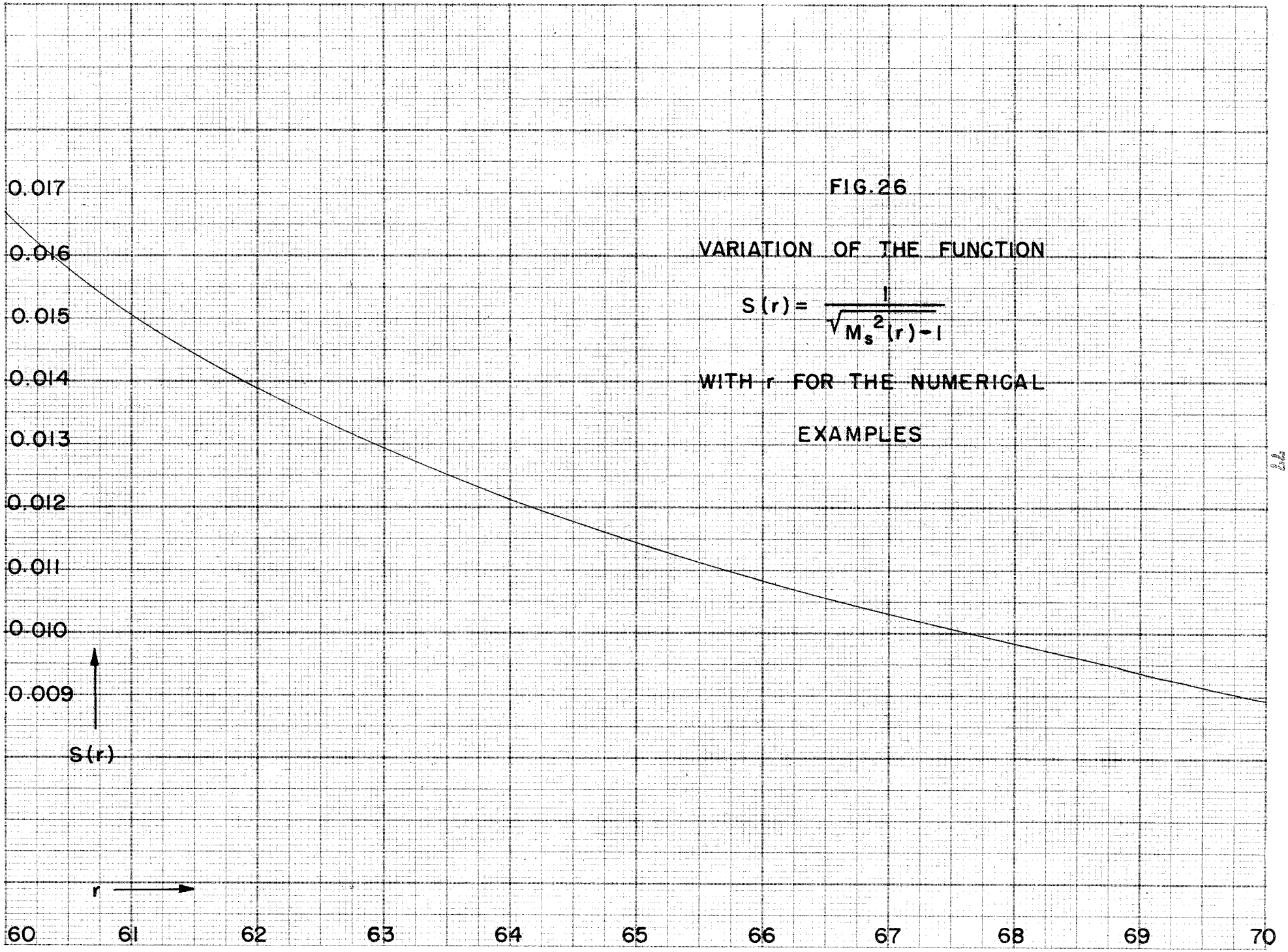

FIG. 26

VARIATION OF THE FUNCTION

$$S(r) = \frac{1}{\sqrt{M_s^2(r) - 1}}$$

WITH r FOR THE NUMERICAL EXAMPLES

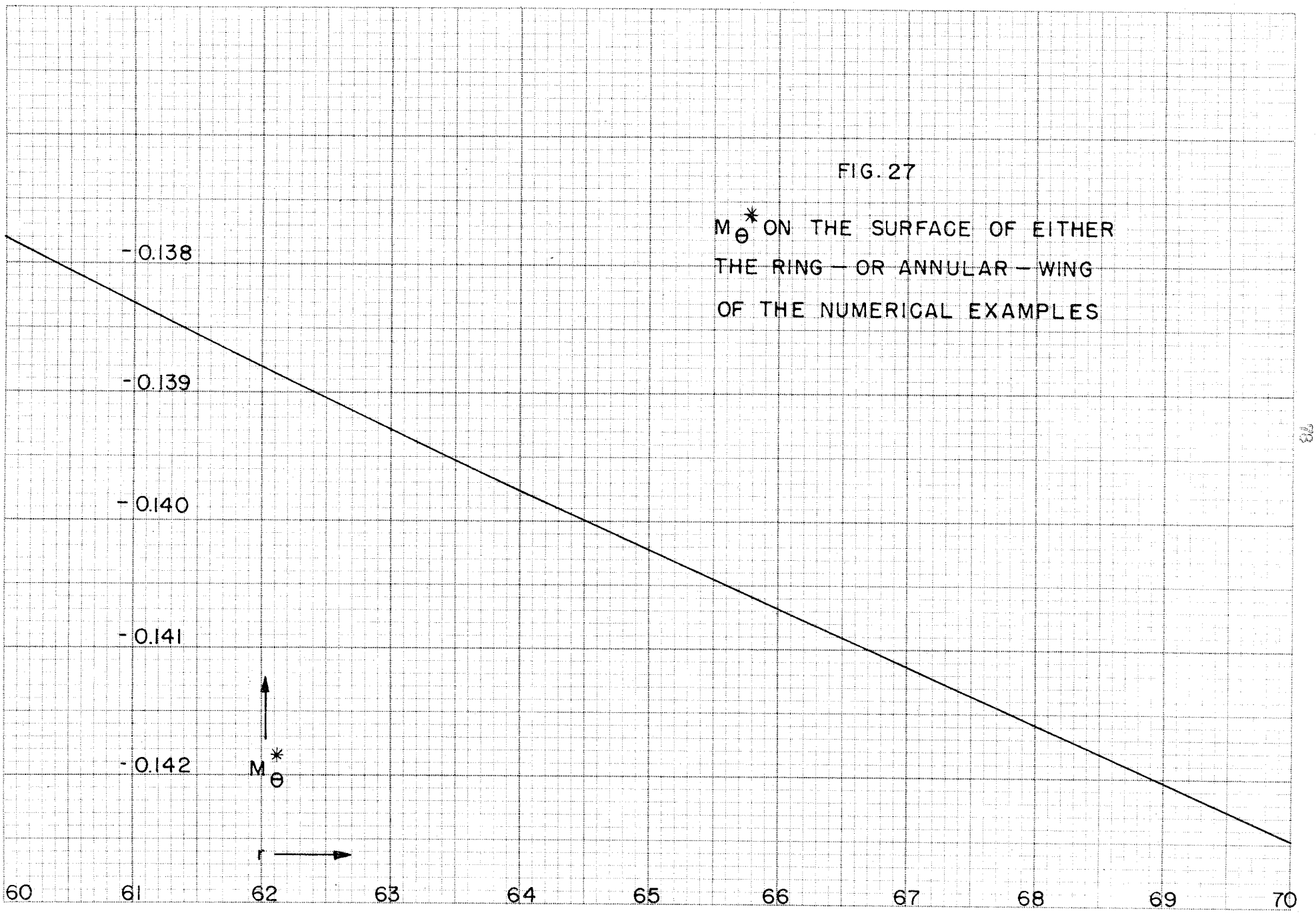

FIG. 27

M_θ^* ON THE SURFACE OF EITHER THE RING — OR ANNULAR — WING OF THE NUMERICAL EXAMPLES

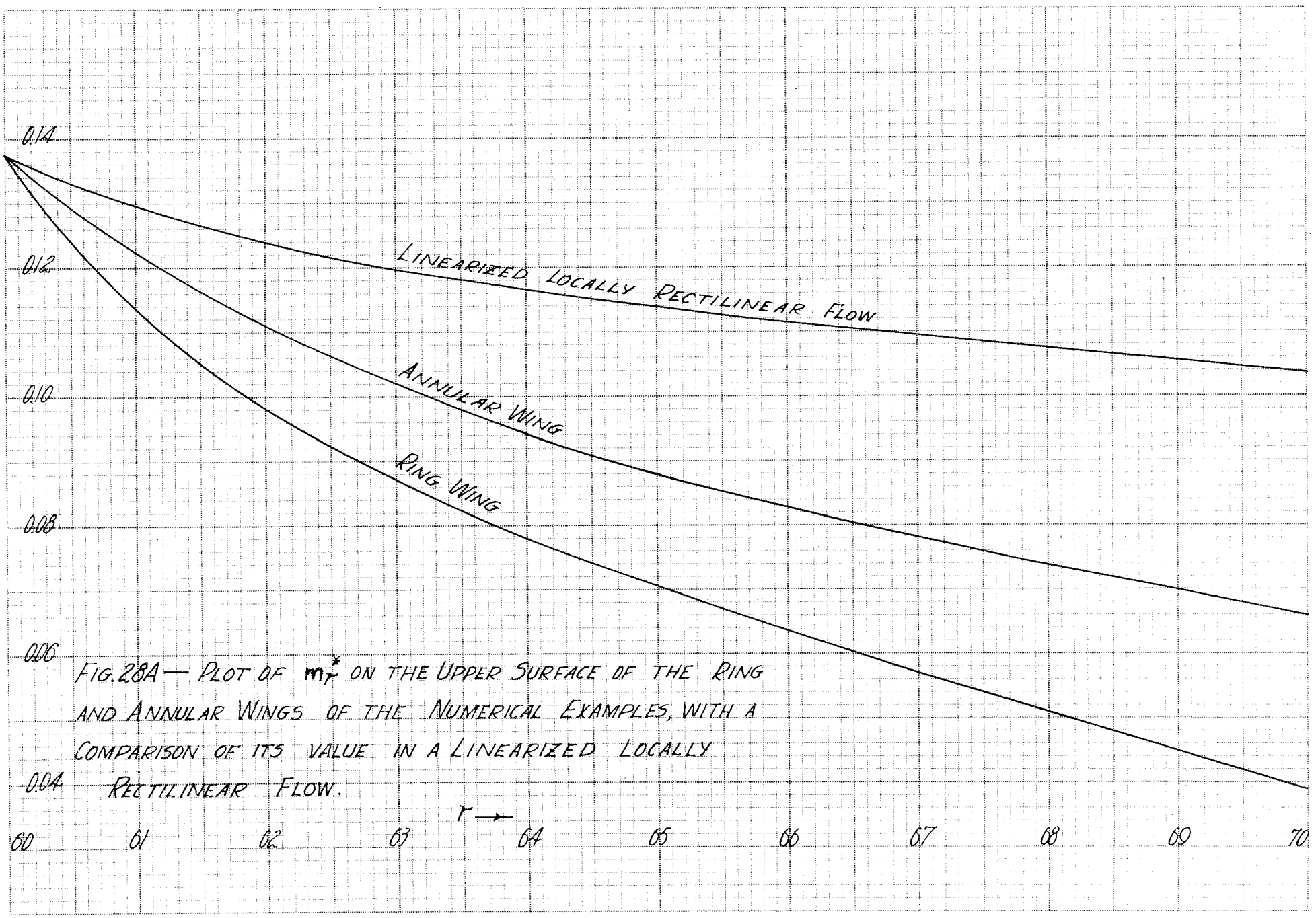

FIG. 28A — PLOT OF m_r^* ON THE UPPER SURFACE OF THE RING AND ANNULAR WINGS OF THE NUMERICAL EXAMPLES, WITH A COMPARISON OF ITS VALUE IN A LINEARIZED LOCALLY RECTILINEAR FLOW.

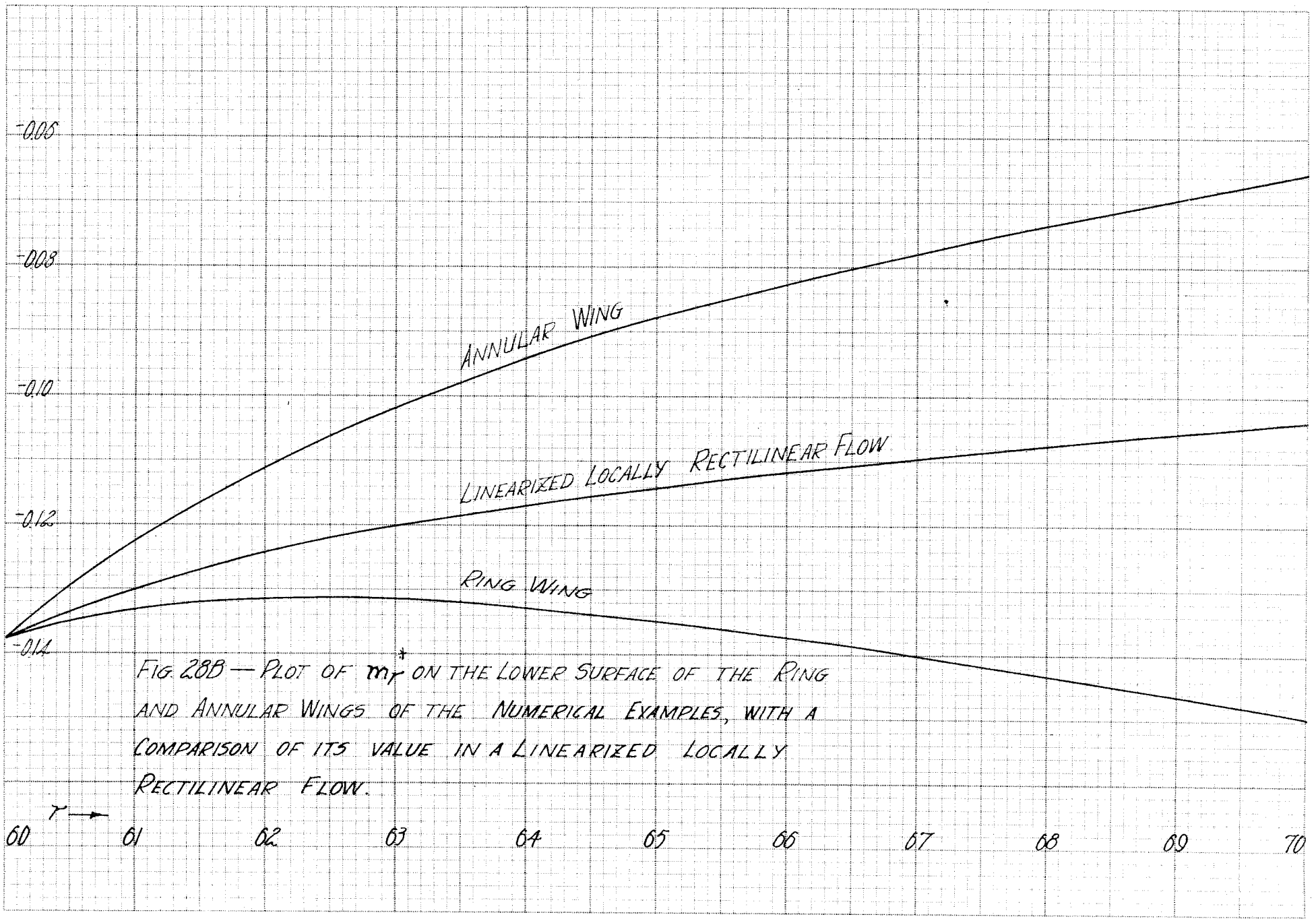

FIG. 28B — PLOT OF $m_r^{\dagger}$ ON THE LOWER SURFACE OF THE RING AND ANNULAR WINGS OF THE NUMERICAL EXAMPLES, WITH A COMPARISON OF ITS VALUE IN A LINEARIZED LOCALLY RECTILINEAR FLOW.

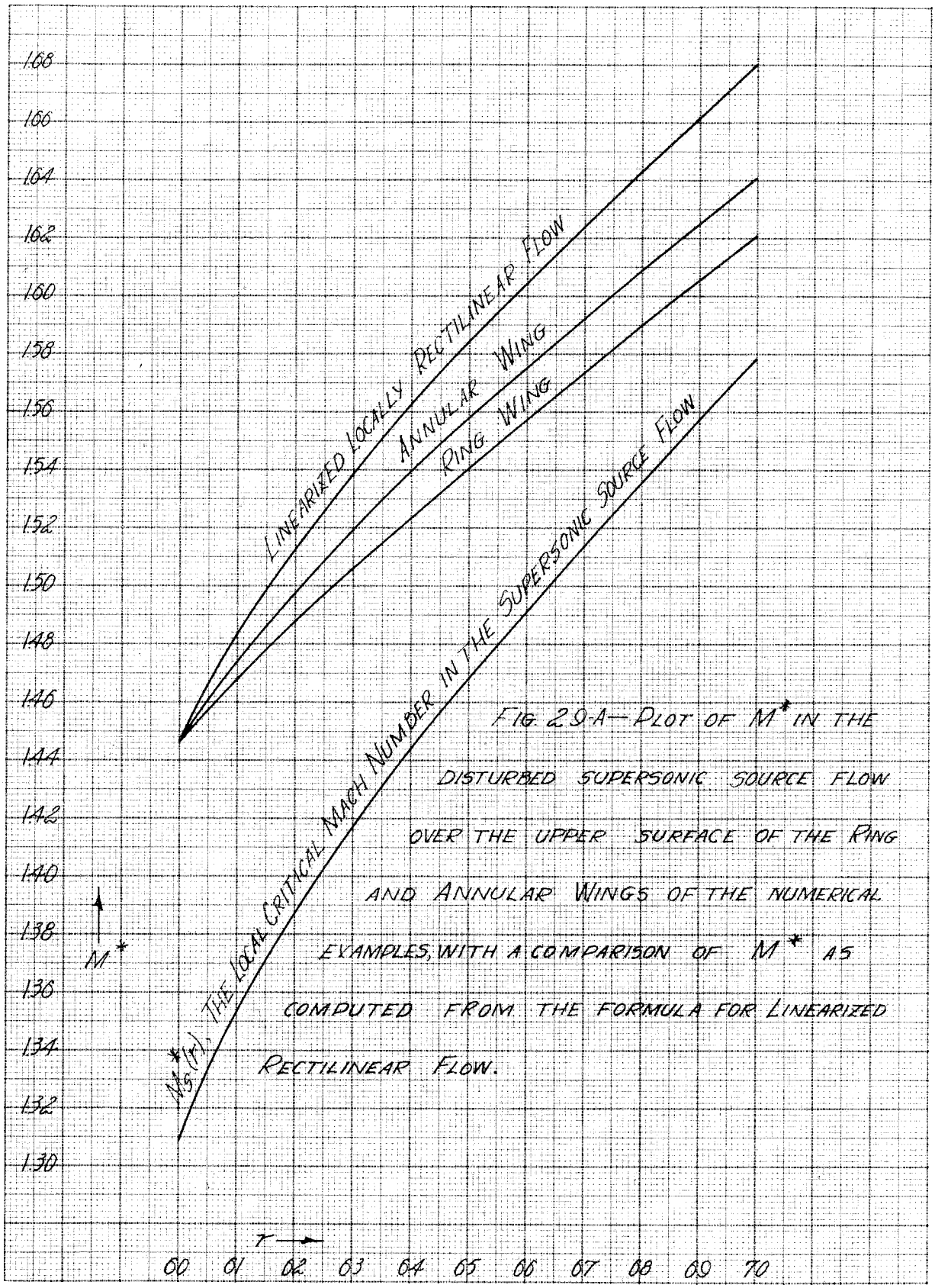

FIG 29-A— PLOT OF M^* IN THE DISTURBED SUPERSONIC SOURCE FLOW OVER THE UPPER SURFACE OF THE RING AND ANNULAR WINGS OF THE NUMERICAL EXAMPLES, WITH A COMPARISON OF M^* AS COMPUTED FROM THE FORMULA FOR LINEARIZED RECTILINEAR FLOW.

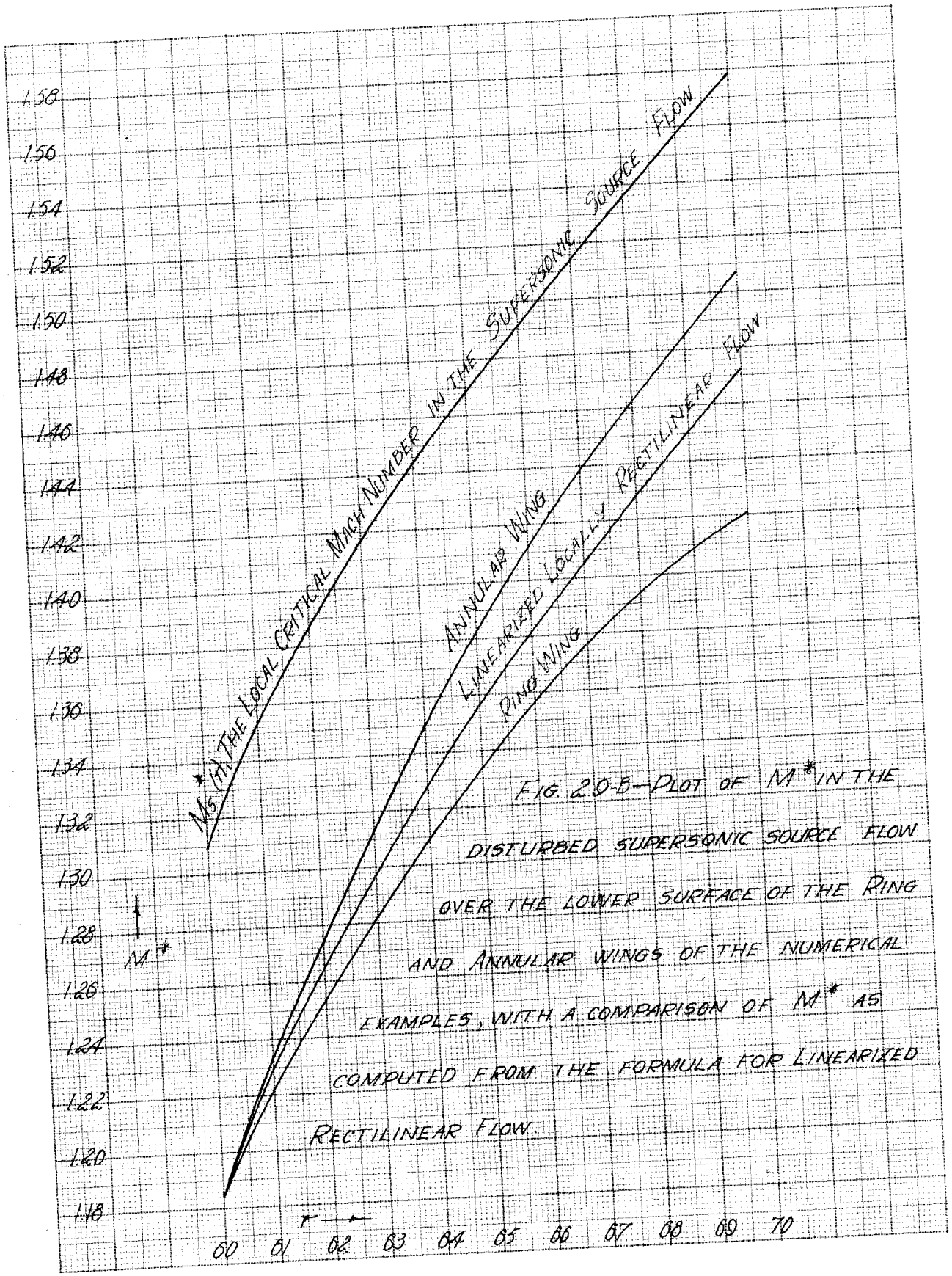

FIG. 2.0-B—PLOT OF M^* IN THE DISTURBED SUPERSONIC SOURCE FLOW OVER THE LOWER SURFACE OF THE RING AND ANNULAR WINGS OF THE NUMERICAL EXAMPLES, WITH A COMPARISON OF M^* AS COMPUTED FROM THE FORMULA FOR LINEARIZED RECTILINEAR FLOW.

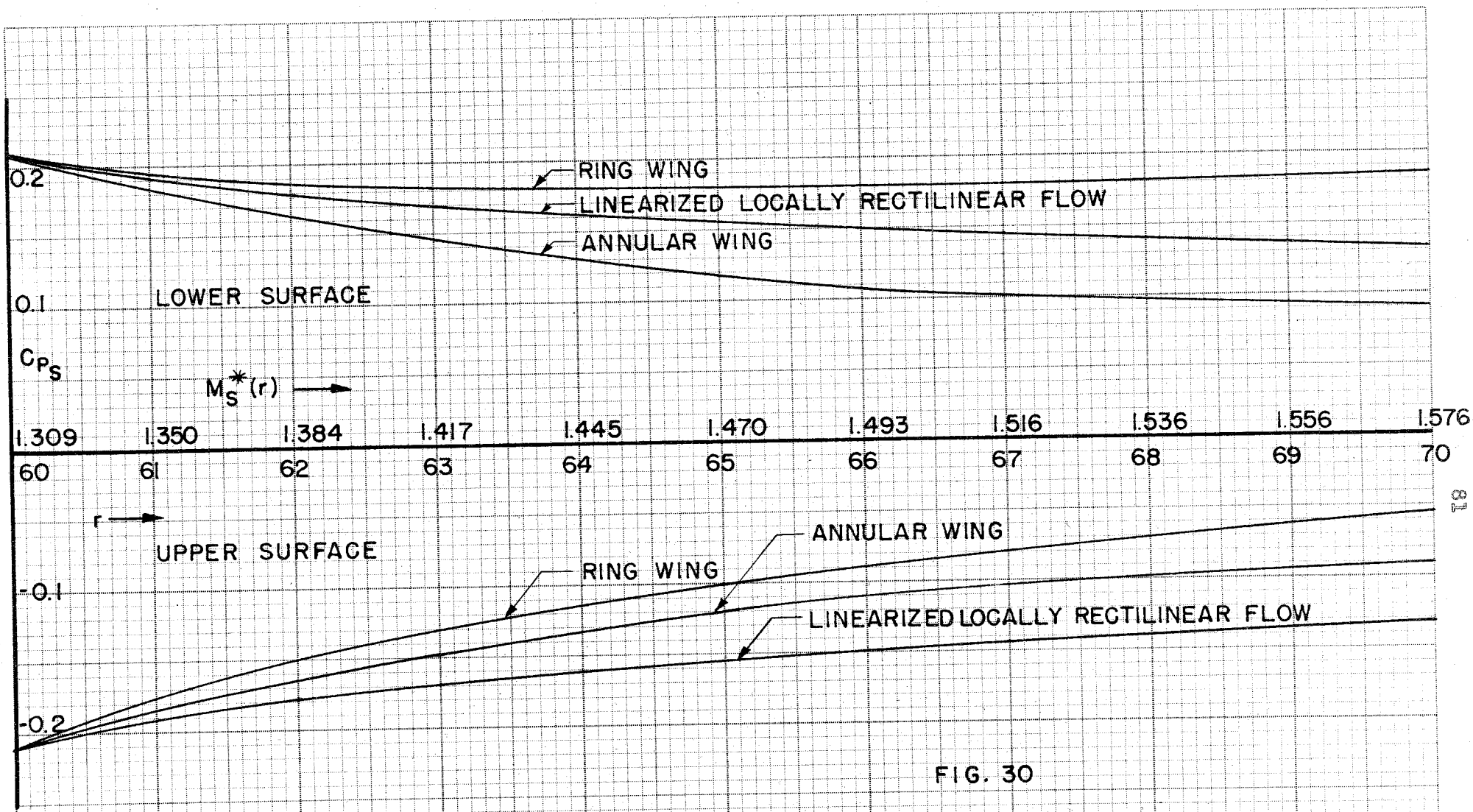

FIG. 30

PRESSURE COEFFICIENTS (BASED ON THE DYNAMIC PRESSURE IN THE SOURCE FLOW) FOR THE RING- AND ANNULAR-WINGS OF THE NUMERICAL EXAMPLES COMPARED WITH THAT OF THE SAME WING IN LINEARIZED LOCALLY RECTILINEAR FLOW

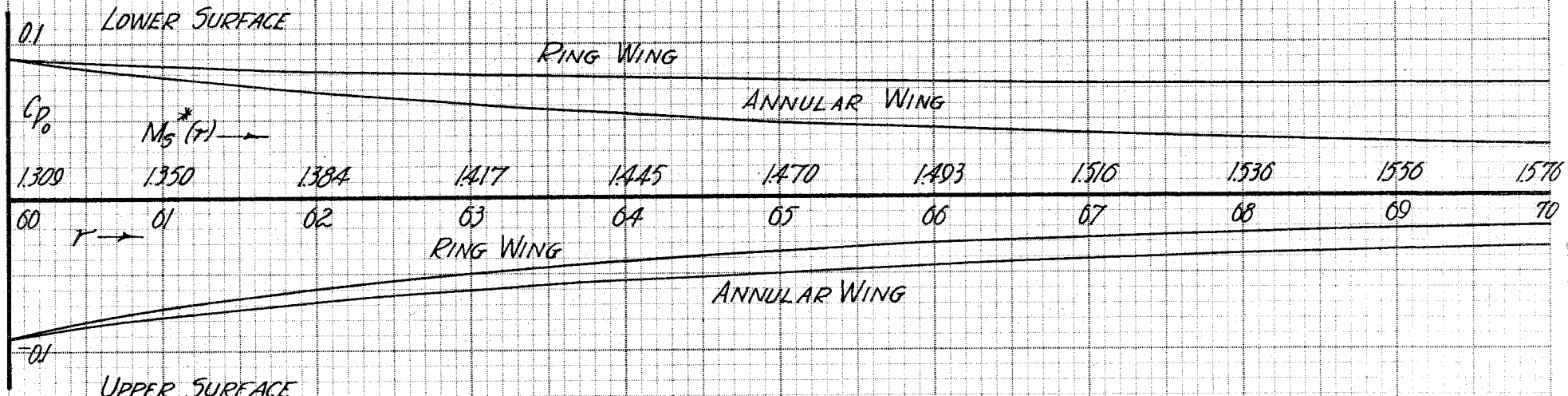

FIG 31 — COMPARISON OF PRESSURE COEFFICIENT C_{P_0} (BASED ON LOCAL STAGNATION PRESSURE) FOR THE RING AND ANNULAR WINGS OF THE NUMERICAL EXAMPLE, COMPUTED FROM THE FORMULA

$$C_{P_0} = \frac{P - P_S}{P_0} = -\frac{2\gamma}{\gamma+1} M_S^*(\tau)\left[1 - \frac{1}{6} M_S^{*2}(\tau)\right]^{2.5} m\tau^*$$